Landsvirkjun

LV-2025-008

Seismic Monitoring in Krafla, Þeistareykir and Námafjall

November 2023 to November 2024

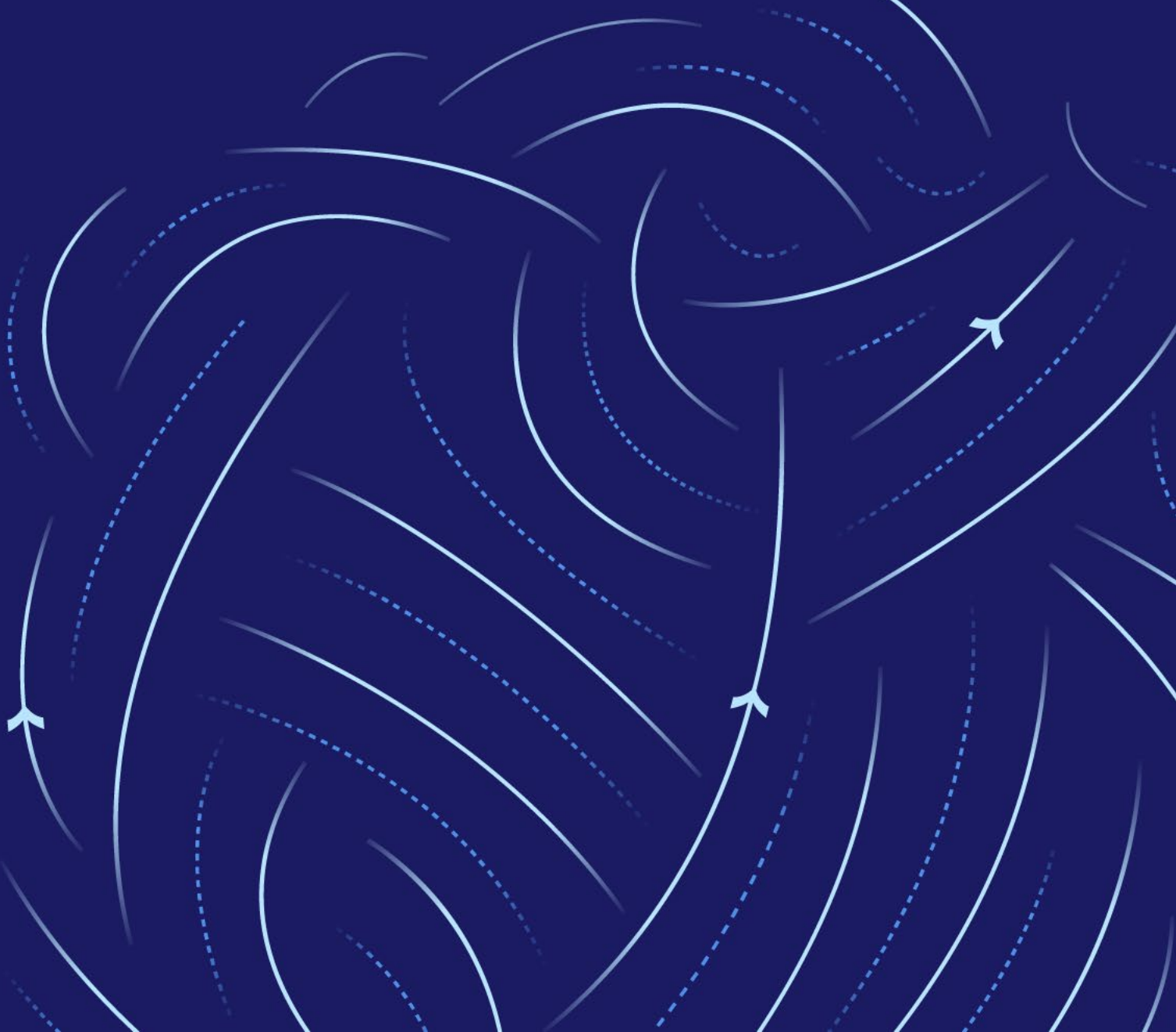

Seismic Monitoring in Krafla, Þeistareykir and Námafjall

November 2023 to November 2024

Höfundar
Egill Árni Guðnason, Þorbjörg Ágústsdóttir, Rögnvaldur Líndal Magnússon and Karl Gunnarsson

Dagsetning
Febrúar 2025

Lykilsíða

Skýrsla LV nr	LV-2025-008	**Dagsetning**	Febrúar 2025
Fjöldi síðna	39	**Upplag**	1
Dreifing	[X] Birt á vef LV	[ ] Opin	[ ] Takmörkuð til [Dags.]
Titill	Seismic Monitoring in Krafla, Þeistareykir and Námafjall: November 2023 to November 2024		
Höfundar/fyrirtæki	Egill Árni Guðnason, Þorbjörg Ágústsdóttir, Rögnvaldur Líndal Magnússon and Karl Gunnarsson / ÍSOR		
Verkefnisstjóri	Anette Kærgaard Mortensen		
Unnið fyrir	Landsvirkjun		
Samvinnuaðilar	–		
Útdráttur	The annual results of earthquake monitoring in the geothermal areas of Krafla, Þeistareykir and Námafjall for the period from 1st of November 2023 to 31st of October 2024 are reported. Around 4,300 earthquakes were located, with the highest concentration of earthquakes in Krafla, and lowest in Námafjall. Micro-seismicity is dominant in all areas, with only two events exceeding ML 2.0. Improvements made to the automatic event processing system are presented. The observed seismicity rate in Krafla and Námafjall is similar to last year, while there is a significant decrease in Þeistareykir, most notably within the Tjarnarás cluster. The decrease coincides with the end of the 2023 inflation episode in Þeistareykir, and is therefore most likely a crustal response to the end of the inflation in the area. Double-couple focal mechanisms are calculated for a total of 241 earthquakes. Diverse faulting styles are inferred, with normal faulting dominant in Krafla, while strike-slip faulting is dominant in both Þeistareykir and Námafjall. 18 earthquakes in Krafla are attributed to non-double-couple mechanisms, both explosive and implosive. Compared to last year, the Vp/Vs ratio remains the same in Krafla, while it varies a little in Þeistareykir and in Námafjall.		
Lykilorð	Krafla, Þeistareykir, Námafjall, earthquakes, seismicity, monitoring, production, re-injection, brittle-ductile, focal mechanism, Vp, Vs, jarðskjálftar, jarðskjálftavirkni, skjálftavirkni, eftirlit, vöktun		

Samþykki verkefnisstjóra
Landsvirkjunar

Anette K. Mortensen

Report no.	Date Veldu dags.	Distribution
ÍSOR-2024/045	December 2024	☒ Open ☐ Closed Dagsetning

Report name / Main and subheadings	Number of copies
Seismic Monitoring in Krafla, Þeistareykir and Námafjall. November 2023 to November 2024.	1
	Number of pages: 39
Authors: Egill Árni Guðnason, Þorbjörg Ágústsdóttir, Rögnvaldur Líndal Magnússon and Karl Gunnarsson	Project manager: Egill Árni Guðnason
Classification of report	Project no.: 24-0061

Prepared for
Landsvirkjun
Cooperators

Abstract

The annual results of earthquake monitoring in the geothermal areas of Krafla, Þeistareykir and Námafjall for the period from 1st of November 2023 to 31st of October 2024 are reported. Around 4,300 earthquakes were located, with the highest concentration of earthquakes in Krafla, and lowest in Námafjall. Micro-seismicity is dominant in all areas, with only two events exceeding M_L 2.0. Improvements made to the automatic event processing system are presented.

The observed seismicity rate in Krafla and Námafjall is similar to last year, while there is a significant decrease in Þeistareykir, most notably within the Tjarnarás cluster. The decrease coincides with the end of the 2023 inflation episode in Þeistareykir, and is therefore most likely a crustal response to the end of the inflation in the area.

Double-couple focal mechanisms are calculated for a total of 241 earthquakes. Diverse faulting styles are inferred, with normal faulting dominant in Krafla, while strike-slip faulting is dominant in both Þeistareykir and Námafjall. 18 earthquakes in Krafla are attributed to non-double-couple mechanisms, both explosive and implosive.

Compared to last year, the Vp/Vs ratio remains the same in Krafla, while it varies a little in Þeistareykir and in Námafjall.

Keywords	ISDN number
Krafla, Þeistareykir, Námafjall, earthquakes, seismicity, monitoring, production, re-injection, brittle-ductile, focal mechanism, Vp, Vs, Landsvirkjun, ÍSOR	Project manager's signature: Egill Árni Guðnason Reviewed by: Arnar Már Vilhjálmsson

ÍSOR

Table of contents

List of figures

List of tables

1 Introduction

Seismic activity is monitored in the three developed high-temperature geothermal areas of the Northern Volcanic Zone, NE Iceland; Krafla, Þeistareykir and Námafjall. The local seismic network is operated by Iceland GeoSurvey (ÍSOR) on behalf of Landsvirkjun (LV), and consists of 21 stations in total, supplemented with 6 stations from the regional seismic network of the Icelandic Meteorological Office (IMO) (Figure 1).

The purpose of the dense seismic network is to monitor seismic activity associated with the utilisation of the three respective geothermal systems, as well as to monitor natural activity in these volcanic environments. The raw seismic data are automatically streamed to ÍSOR, where they are processed in real-time. All detected earthquakes are manually reviewed and refined. The operation of the seismic network since 2006 has provided a large and interesting dataset of earthquakes, and results have been published in both yearly reports by ÍSOR (e.g., Guðnason et al., 2023a and references therein) and in an overview report, where the entire catalogue (2006-2022) was reprocessed (Guðnason et al., 2023b).

This annual report presents results of earthquake monitoring in the geothermal areas of Krafla, Þeistareykir and Námafjall, for the period from the 1st of November 2023 to the 31st of October 2024. In line with the project contract, the report contains e.g., refined earthquake locations, focal mechanisms of selected earthquakes and a calculation of the Vp/Vs ratio for all three areas.

2 The seismic network

The LV/ÍSOR seismic network consists of 21 permanent stations (Figure 1). The geometry of the seismic network in the Krafla and Námafjall areas has remained the same since 2015 and 2017, respectively, while the seismic network in Þeistareykir was expanded in 2021, with three stations from the German Research Centre for Geosciences (GFZ) added to the permanent LV/ÍSOR seismic network.

3 Seismic characteristics

From the 1st of November 2023 to the 31st of October 2024, a total of 4,311 earthquakes were detected and located in the Krafla, Þeistareykir and Námafjall geothermal areas, and surroundings (Figure 1). For comparison, the regional seismic network of the Icelandic Meteorological Office (IMO) in Iceland located 509 earthquakes in the same area during this period, or ~12%, similar to previous years.

Rate

There are only small variations in the observed seismicity rate in the Krafla and Námafjall areas, compared to last year (Guðnason et al., 2023a), while there is a significant decrease in Þeistareykir, further discussed in chapter 3.2. As before, the number of earthquakes in Krafla is higher compared to Þeistareykir and Námafjall. In total, 3,526 earthquakes were located in the Krafla area (293/month on average, compared to 282/month last year), 622 earthquakes in the Þeistareykir area (52/month on average, compared to 113/month last year) and 125 earthquakes

in the Námafjall area (10/month on average, compared to 8/month last year). A small number of events are located around the western caldera rim of Krafla, and along the volcanic rift zone north of Krafla and southeast of Þeistareykir, which are outside the scope of this report.

Processing

All earthquakes were automatically detected and located in real-time using the SeisComP software (https://www.seiscomp.de/), and all were manually reviewed and refined. This year, the *scrttd* SeisComP module (https://docs.gempa.de/scrtdd/current), which was first introduced as part of ongoing development at ÍSOR in Guðnason et al. (2023b), was activated as part of the automatic event processing system. This module relocates earthquake solutions discovered by other locators, e.g., *scanloc* (https://docs.gempa.de/scanloc/current/apps/scanloc.html), using a double-difference method, as well as using waveform cross-correlation to refine, or in some cases add phase arrivals. Currently, *scrttd* runs in single event mode, where a single event is relocated with respect to a previously created background catalogue of earthquakes. The performance of the *scrttd* module is further described in Appendix A.

For the purpose of this report, all manually reviewed earthquake locations were refined using the NonLinLoc algorithm (Lomax et al., 2000) in order to improve the earthquake location, which takes the absolute elevation of the seismic stations into account in the location routine. All earthquakes are located using a gradient version of the ÍSOR velocity model, based on processing and interpretation of refraction surveys performed in Krafla in 1961-1963 and 1971-1973 (Ágústsson et al., 2011), except earthquakes in the Þeistareykir area, which are located using a gradient local velocity model for the area (Guðnason and Ágústsdóttir, 2021).

Magnitudes and seismicity rate

All recorded earthquakes are small, with 99% of $M_L < 1.0$. Only two events exceed M_L 2.0 (Figure 1), both originating at around 2 km depth within the Krafla well field (Figure 2). As before, seasonal fluctuations are observed in the magnitude range in all three geothermal areas (Figures 3, 5 and 8), whereas this signal is strongest in Krafla. The daily seismicity rate in Krafla and Námafjall is slightly greater during the winter months throughout May, while in Þeistareykir, the increased seismicity rate observed last year (Guðnason et al., 2023a), coinciding with a period of inflation, continued until approximately the end of last year, 2023, further discussed in chapter 3.2. The overall sensitivity of the seismic network is higher during the summer months in all areas, with smaller magnitude events detected, most likely due to better weather conditions.

Brittle-ductile transition

As before, the brittle-ductile transition (BDT) in the three geothermal areas is rather variable from one area to the other, with no obvious changes compared to previous years (Figure 1). In particular, it domes up to shallowest depths below the Krafla well field, but also below Mt. Bæjarfjall in Þeistareykir and to some extent below the Námafjall well field. In the following chapters, 3.1-3.3, results are presented for individual geothermal areas separately.

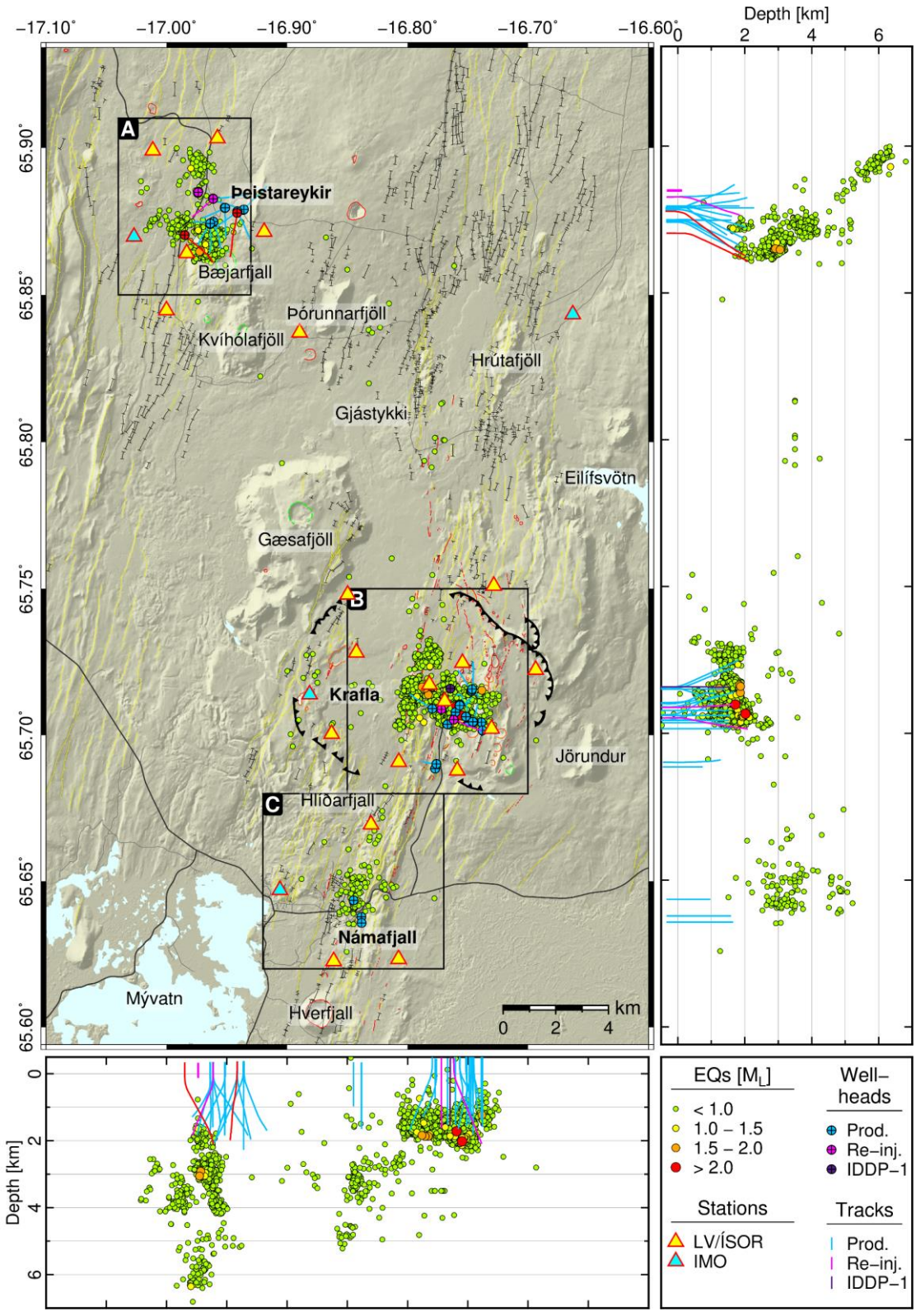

Figure 1. *Refined manual earthquake locations of 4,311 earthquakes in the Krafla, Þeistareykir and Námafjall geothermal areas during the study period, in map and depth view. Earthquake locations are colour-coded according to magnitude. See legend for different seismic stations, wellheads and well trajectories. Mapped geological structures are from Sæmundsson et al. (2012). Main roads are in black, and main landmarks referenced in the text are shown on the map. Black boxes mark the outlines of the zoomed-in view of each geothermal area as shown in Figures 2, 4 and 7.*

3.1 Krafla

Earthquake activity in the Krafla geothermal area is shallow, with 94% of earthquakes confined to the depth range of 1-2 km b.s.l. during the study period (Figure 2). The activity is confined to at least three spatially separated clusters (Schuler et al., 2015a), which are separated by areas of little or no seismicity.

Two of the three clusters originate within the fissure swarm transecting Leirhnjúkur. Different from last year (Guðnason et al., 2023a), seismicity is almost absent from the cluster of deeper earthquakes (~2.5-3 km) that originates furthest to the SSW within the fissure swarm of Krafla, which has been sporadically active throughout the years (Guðnason et al., 2023b). Earthquake activity within the fissure swarm is around 21% of the total number of earthquakes in Krafla during the study period (Figure 3 and Figure B1 in Appendix B) (similar to last year).

The third and largest cluster in the Leirbotnar-Suðurhlíðar area is the most seismically active during the study period and confined to the Krafla geothermal well field, with around 79% of located earthquakes in the area (Figure 3 and Figure B1 in Appendix B). The micro-seismic activity in this area is more or less constant between ~1-2 km depth, with the highest seismicity rate during the winter months, and a higher daily rate of earthquakes in between, but no specific earthquake swarms are observed during the past year.

Magnitudes

Magnitudes in Krafla during the study period range from M_L -0.5 to 2.1 (Figure 3). Earthquakes of $M_L > 1$ are within 1% of the total catalogue in Krafla, and the majority of these "larger" earthquakes are confined to the deeper end of the depth range, with the largest earthquakes during the study period occurring within the well field cluster (Figure 2). This indicates that the crust in Krafla is strongest, or under most strain, close to the shallow brittle-ductile transition. As before, seasonal fluctuations are observed in the magnitude distribution, with smaller earthquakes detected during summer, than during winter.

Spatial and temporal distribution

Overall, the depth distribution of earthquakes in Krafla suggests that the BDT is at around 2 km depth (Figure 2). Previous work has attempted to link the BDT to a specific temperature range of 550 ± 100°C in Iceland, based on laboratory experiments on Icelandic basalts (Violay et al., 2012). The higher temperatures expected at the BDT in Krafla are confirmed by the two wells that encountered magma during drilling, i.e., wells KJ-39 and IDDP-1, drilled down to the BDT at 2 km depth (Árnadóttir et al., 2009; Mortensen et al., 2014).

Looking at the micro-seismic activity in Krafla as i) depth and ii) longitude as a function of time (Figure B2 in Appendix B), it is evident that the activity is in general rather constant, in particular within the well field. Due to a local weaker crust in Krafla, (high *b*-value), stress is released early by numerous, small earthquakes, and thus, earthquake swarms or large magnitude earthquakes are rarely observed (e.g., Guðnason et al., 2021).

Rate

During the study period, days of higher seismicity rate rarely occur all in one swarm on a single fault, or in a confined area (Figures 3 and 4). As before, small-amplitude aftershocks are occasionally observed in the seismic waveform of larger-amplitude earthquakes, but more frequently, earthquakes with similar waveforms and magnitudes, separated only by a few seconds are observed (Guðnason et al., 2021), referred to as multiplets by Schuler et al. (2016).

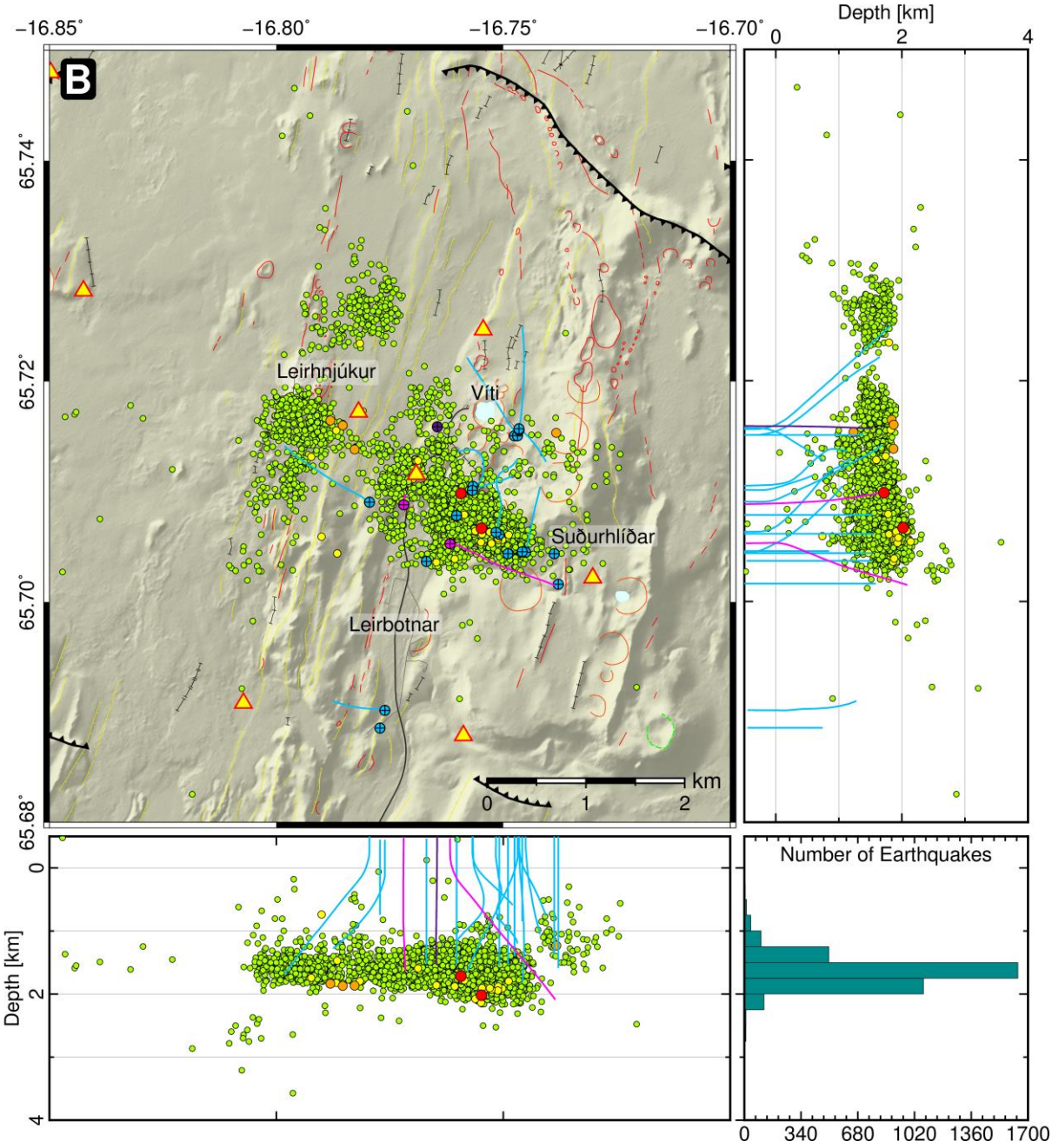

Figure 2. *Refined manual earthquake locations of 3,526 earthquakes in the Krafla geothermal area (box B in Figure 1) during the study period, in map and depth view. See legend and figure caption from Figure 1 for references to the map.*

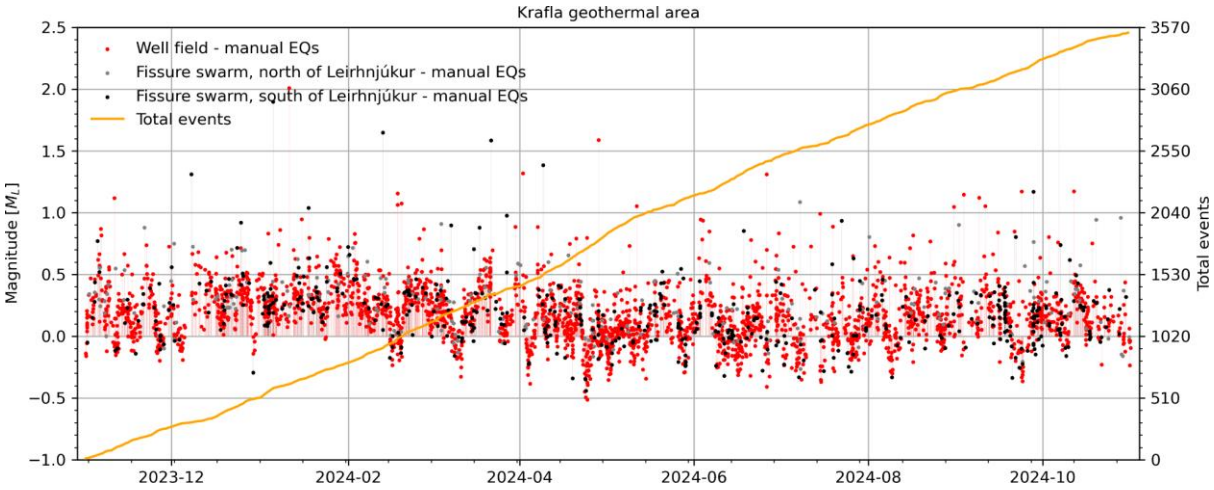

Figure 3. *Time vs. magnitude (M_L) plot of the 3,526 located earthquakes in the Krafla geothermal area (box B in Figure 1) during the study period. Manual earthquakes are shown as different coloured dots, referring to the three different clusters of i) the well field (red) and the fissure swarm, ii) north (grey) and iii) south (black) of Leirhnjúkur. The orange line shows the cumulative number of earthquakes. The three clusters are presented in more detail in Figure B1 in Appendix B.*

3.2 Þeistareykir

Earthquake activity in the Þeistareykir geothermal area occurs, as before, in more or less three spatially separated clusters during the study period; below Mt. Bæjarfjall, in Randir/Hitur and in Tjarnarás (Figure 4). The largest of the three is the well-defined cluster of earthquakes below the northwest flanks of Mt. Bæjarfjall, with majority of earthquakes occurring within the depth range of around 2.5-3.5 km. This cluster most likely represents an up-doming of the BDT in Þeistareykir, where high temperatures are expected (further discussed in e.g., Guðnason et al., 2023b). Slightly deeper earthquakes (~4 km depth) occur just east of this cluster, below the northern flanks of Mt. Bæjarfjall, while a tiny cluster of earthquakes is active at around 1.5-2 km depth just northwest of Mt. Bæjarfjall, where geothermal manifestations are observed on the surface. The other two active clusters in Randir/Hitur and in Tjarnarás are smaller than the Mt. Bæjarfjall cluster, and confined to greater depths, > 3.5 km (Figure 4).

Magnitudes

Magnitudes in Þeistareykir during the study period range from M_L -0.9 to 1.8 (Figure 5). Earthquakes of $M_L > 1.0$ are around 1% of the total catalogue in Þeistareykir, and two of the largest earthquakes during the study period, of M_L 1.5 and 1.8, both occur at around 3 km depth below the western flanks of Mt. Bæjarfjall (Figure 4). As in Krafla, seasonal fluctuations are observed in the magnitude distribution, with smaller earthquakes detected during summer, than during winter.

Spatial and temporal distribution

Looking at the micro-seismic activity in Þeistareykir as i) depth and ii) latitude as a function of time (Figure 6), it is evident that that the activity within the Mt. Bæjarfjall cluster is in general rather

constant. The activity within the Randir/Hitur and Tjarnarás clusters is more scattered in time, with an observed decrease in activity within both clusters compared to last year, further discussed below.

Overall, the depth distribution of earthquakes in Þeistareykir (since late 2014) suggests that the BDT is shallowest at ~3.5 km depth below the northwest flanks of Mt. Bæjarfjall, coinciding with a part of the main production field (Figure 4) (Guðnason et al., 2023b). The BDT deepens below the northern flanks of Mt. Bæjarfjall, and within the Randir/Hitur cluster, to ~4 km depth, deepening further within the fissure swarm towards north to 5.5-7 km depth. As before, earthquake activity is shallowest at ~2 km depth within the tiny cluster of earthquakes just northwest of Mt. Bæjarfjall.

Rate

Seismicity in Þeistareykir is thought to be mainly of natural origin, as discussed in e.g., Guðnason et al. (2023b) and Schuler et al. (2015b), as it has prevailed in more or less the same three separate clusters since years before utilisation of the geothermal field started in 2017.

During the study period, there is an overall decrease in seismicity rate observed in the Þeistareykir area compared to last year, notably within all three clusters (Figures 5, 6 and C1 in Appendix C) (Guðnason et al., 2023a). The largest decrease is observed within the Tjarnarás cluster and the least decrease within the Mt. Bæjarfjall cluster. Last year, the observed increase coincided with the start of an inflation in Þeistareykir at the beginning of 2023, with the centre of uplift approximately 2.5 km west of the Þeistareykir power plant, an actual uplift rate of ~20-25 mm/yr, and an inferred source depth of ~5 km (Drouin, 2023; Gudnason et al., 2024). The uplift seems to have stopped at around the end of last year (Drouin, 2024), which coincides with the decreased seismicity rate observed within both the Randir/Hitur and the Tjarnarás clusters during the study period (Figures 5, 6 and C1 in Appendix C). Thus it is concluded that the increased activity last year, and the decreased activity this year back to more or less normal background levels, is of natural origin, and most likely a crustal response to the inflation period in the Þeistareykir area.

Due to a local weaker crust in Þeistareykir (high *b*-value), stress cannot build up to very high levels but is instead released early by numerous, small earthquakes (Guðnason et al., 2021). However, different to Krafla, occasional small, short-lived earthquake swarms do occur in Þeistareykir (Figures 5, 6 and C1 in Appendix C). During the study period, the most pronounced swarm of 24 earthquakes per day occurred below the northern flanks of Mt. Bæjarfjall on the 21st of September, 2024.

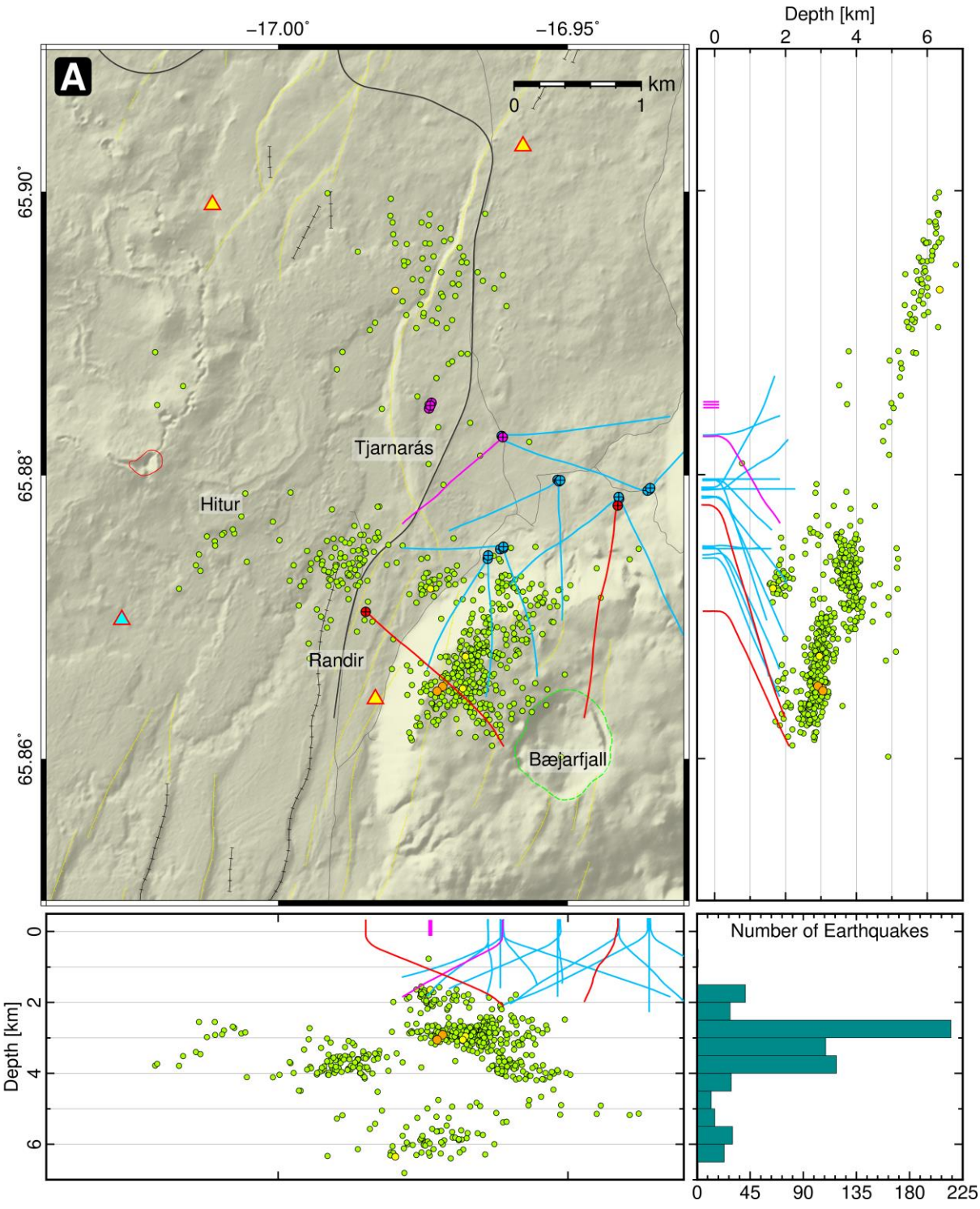

Figure 4. *Refined manual earthquake locations of 622 earthquakes in the Þeistareykir geothermal area (box A in Figure 1) during the study period, in map and depth view. See legend and figure caption from Figure 1 for references to the map. The two most recently drilled wells, ÞG-19 and ÞG-20, are highlighted in red colour.*

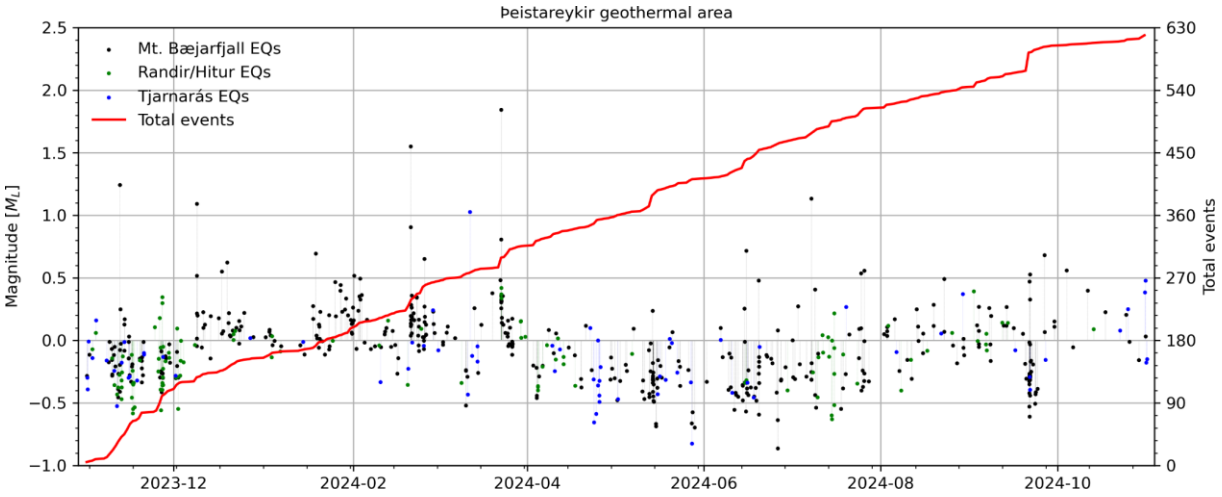

Figure 5. *Time vs. magnitude (M_L) plot of the 622 located earthquakes in the Þeistareykir geothermal area (box A in Figure 1) during the study period. Manual earthquakes are shown as different coloured dots, referring to the three different clusters of Mt. Bæjarfjall (black), Randir/Hitur (green) and Tjarnarás (blue) (each cluster is presented separately in igure C1 in Appendix C). The red line shows the cumulative number of earthquakes.*

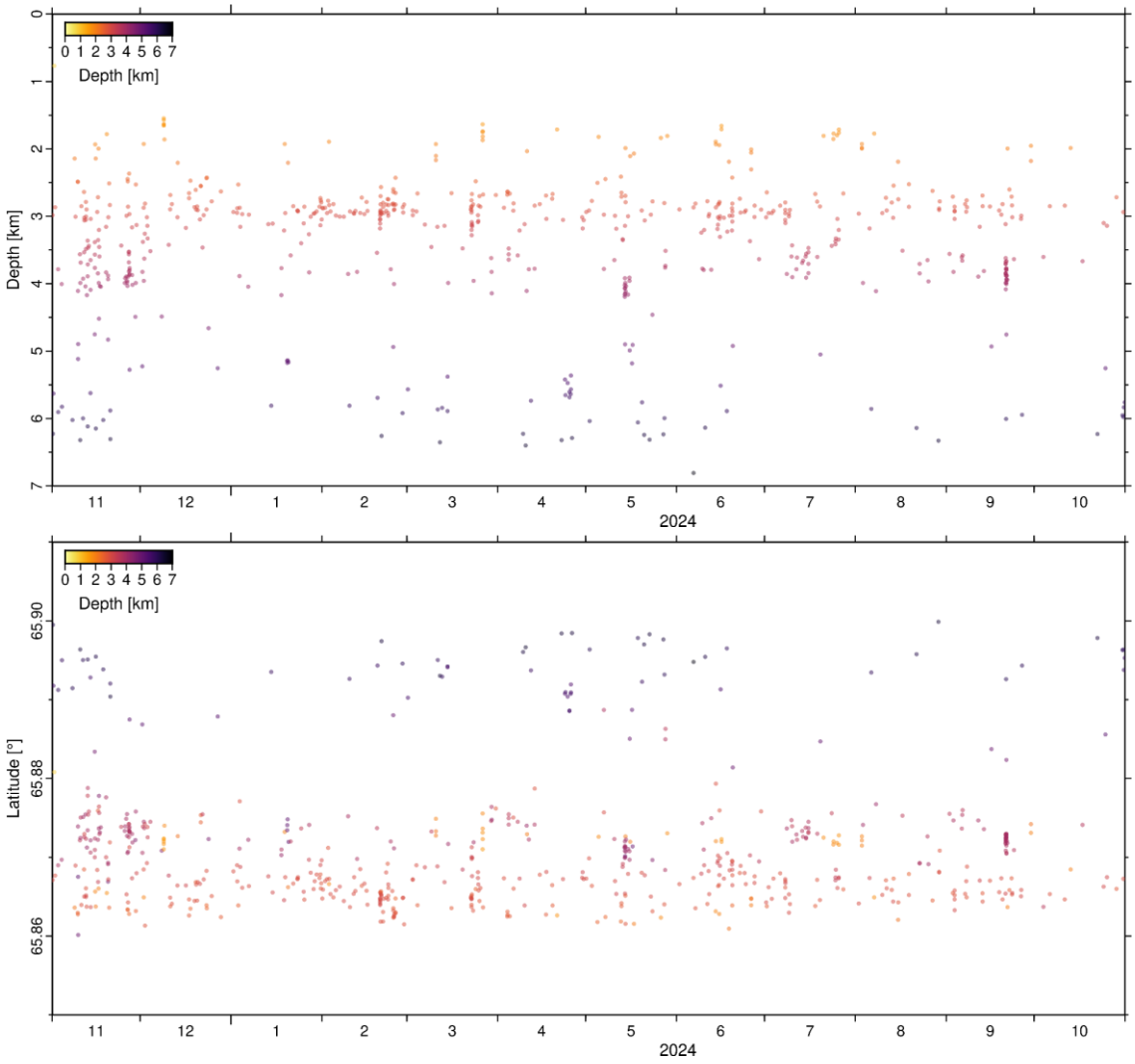

Figure 6. *Time vs. depth (top) and latitude (bottom) of located earthquakes in the Þeistareykir geothermal area (box A in Figure 1) during the study period. Earthquakes are colour-coded by depth.*

3.3 Námafjall

As before, earthquake activity in the Námafjall geothermal area occurs in a rather scattered cluster within the depth range of 2-5 km during the study period (Figure 7). The majority of earthquakes are confined to one cluster within the well field, i.e., below well B-09, at a limited depth interval of 2.5-3.5 km. Other events during the study period are more scattered and fade north into the fissure swarm.

Magnitudes

Magnitudes in Námafjall during the study period range from M_L -0.4 to 0.8 (Figure 8). As in Krafla and Þeistareykir, seasonal fluctuations are observed in the magnitude distribution, although the earthquakes are few, with smaller earthquakes detected during summer than during winter.

Rate

The low micro-seismic activity in the Námafjall geothermal area during the study period is characterised by a rather constant activity, although the rate is slightly higher during the winter months throughout May (Figure 8).

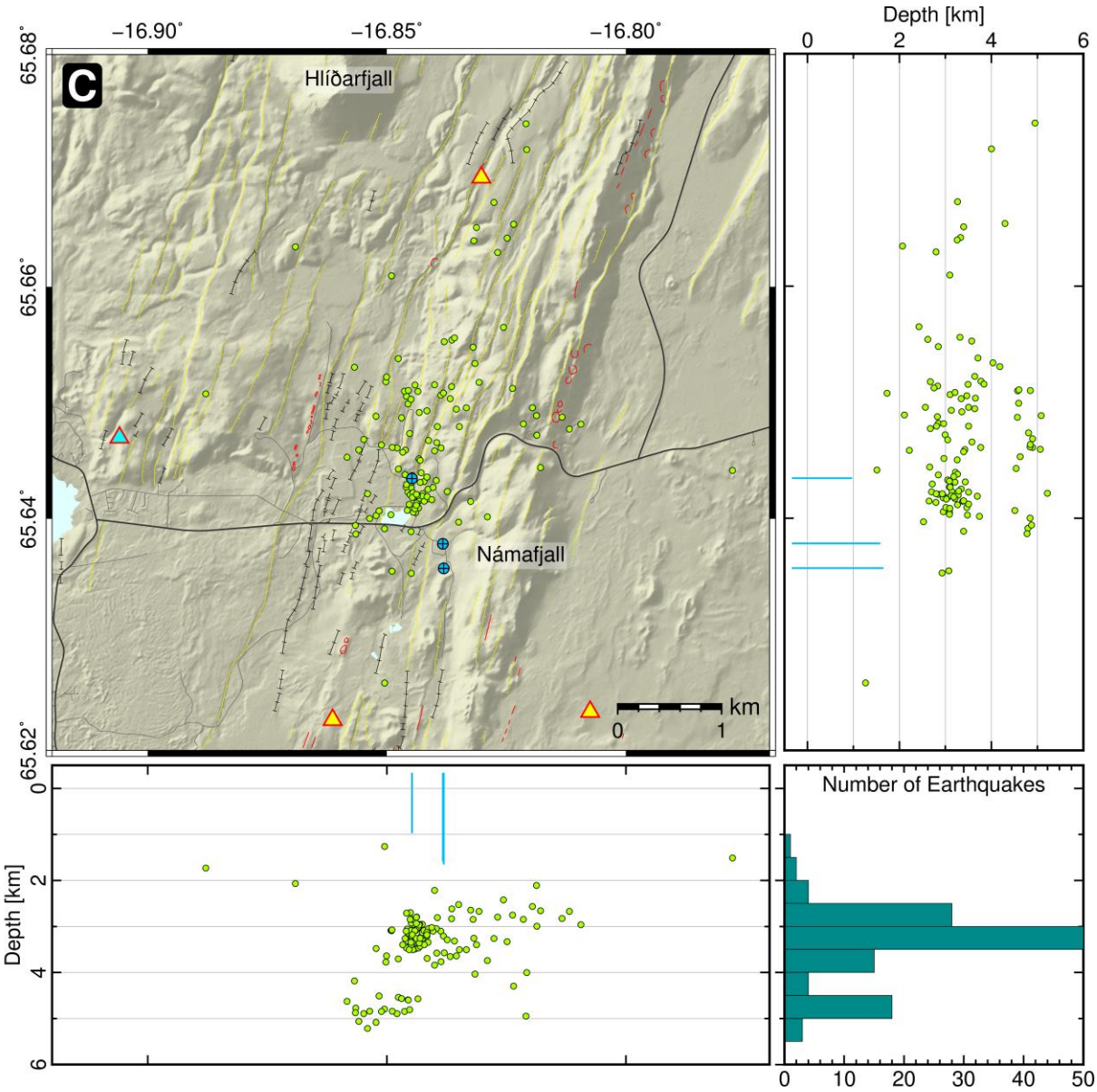

Figure 7. *Refined manual earthquake locations of 125 earthquakes in the Námafjall geothermal area (box C in Figure 1) during the study period, in map and depth view. See legend and figure caption from Figure 1 for references to the map.*

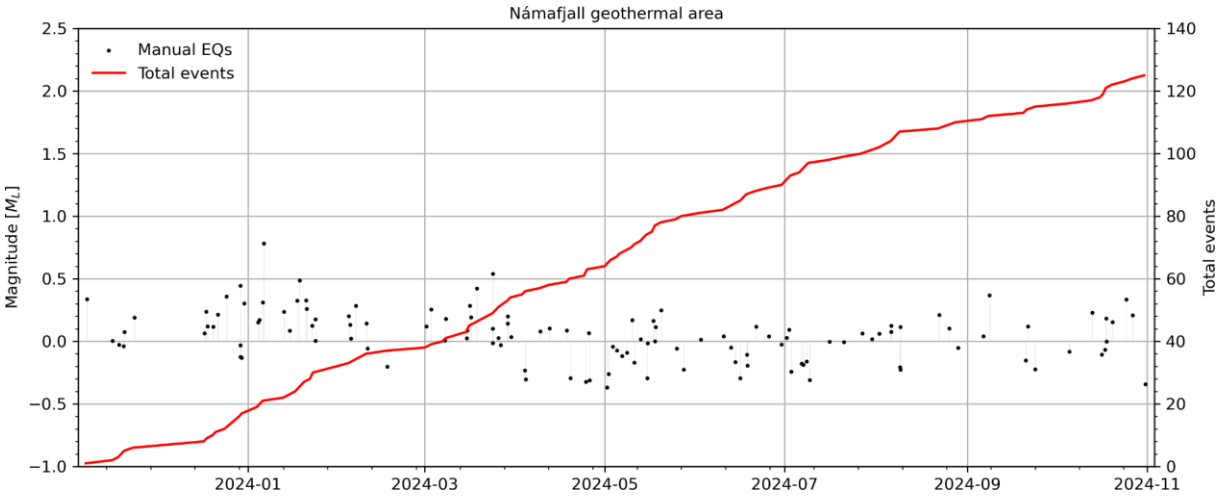

Figure 8. *Time vs. magnitude (M_L) plot of the 125 located earthquakes in the Námafjall geothermal area (box C in Figure 1) during the study period. Manual earthquakes are shown as black dots, and the red line shows the cumulative number of earthquakes.*

4 Focal mechanisms

Focal mechanisms presented in this report (further explained e.g., in Guðnason et al., 2023a) are calculated using the MTfit inversion software (Pugh and White, 2018). These are full moment tensor inversions using the P-wave polarity phases and take-off angles in the calculations. The focal mechanisms are displayed on maps as “beach ball” symbols, which is the stereographic projection on a horizontal plane of the lower half of an imaginary, spherical shell (the focal sphere) surrounding the earthquake source, where a coloured quadrant represents upward motion at a station and a white quadrant represents downward motion.

The T-axis (tension-axis, minimum compression), P-axis (pressure axis, maximum compression) and N-axis (consistent with the intersection of the nodal planes) are orthogonal to each other. T- and P- axes are deviated 45° from the nodal planes. Their azimuth and plunge give additional information on the direction and inclination of faults. The plane defined by the T- and P-axes also contains the normal vectors to the nodal plane, whereof one is the slip vector.

A total of 241 well constrained double-couple focal mechanisms were analysed during the study period; or 168 in Krafla, 55 in Þeistareykir and 18 in Námafjall (Figure 9). To investigate the focal mechanisms in each area in more detail, a Frohlich categorisation of the mechanisms is used, to give a better overview of the focal mechanism distribution (Figure 10). It is a triangle diagram, where the vertices represent normal, strike-slip and reverse faulting focal mechanisms using the plunge of the N-, T- and P-axis (Frohlich, 1992). The focal mechanisms in each area are coloured according to the categorisation, i.e., red colour denotes normal faulting, purple strike-slip faulting, orange reverse faulting, and the oblique events are denoted in yellow (Figures 11-16).

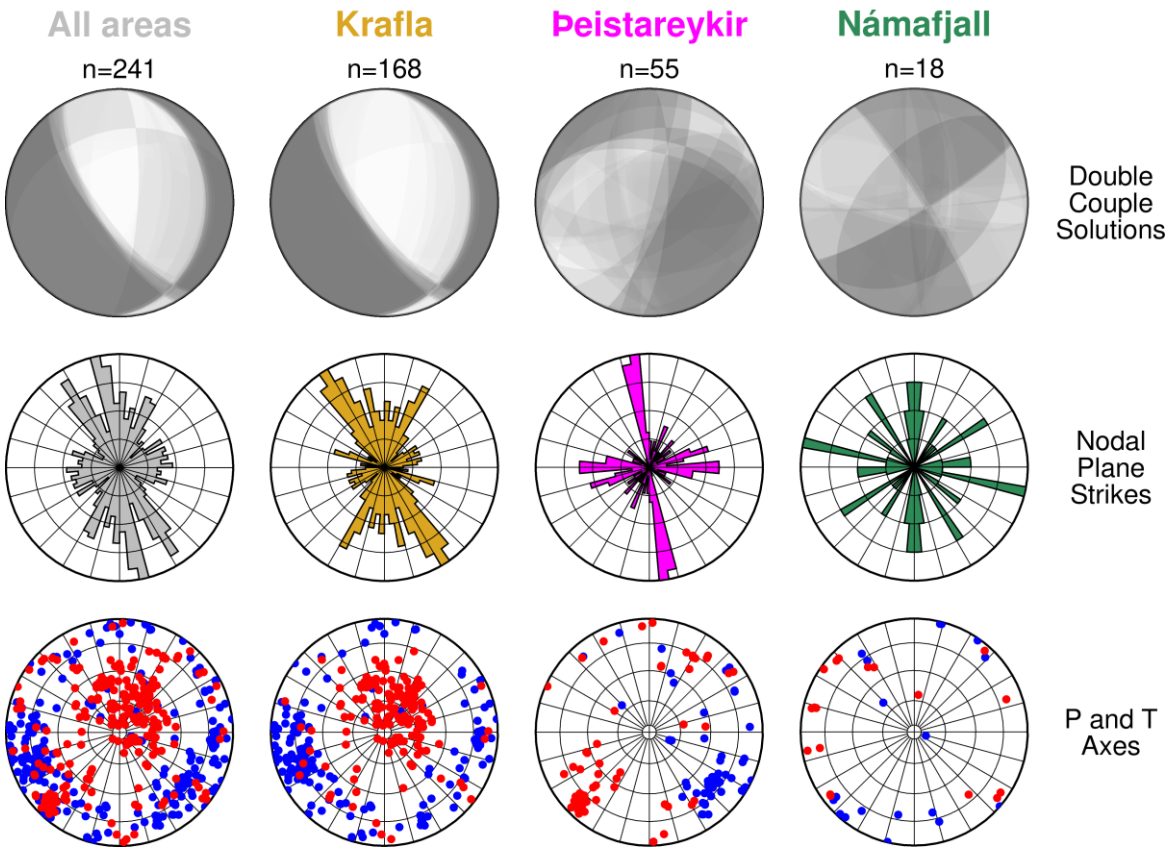

Figure 9. *Graphic summary of all 241 double-couple focal mechanisms located in the Krafla, Þeistareykir and Námafjall geothermal areas during the study period, where n equals number of earthquakes in each group. Top row: all focal mechanisms (white dilatation, grey compression), middle row: strike orientation of all nodal planes, bottom row: orientation of the maximum (P-axis (pressure-axis), red dots) and minimum (T-axis (tension-axis), blue dots) compressive stress.*

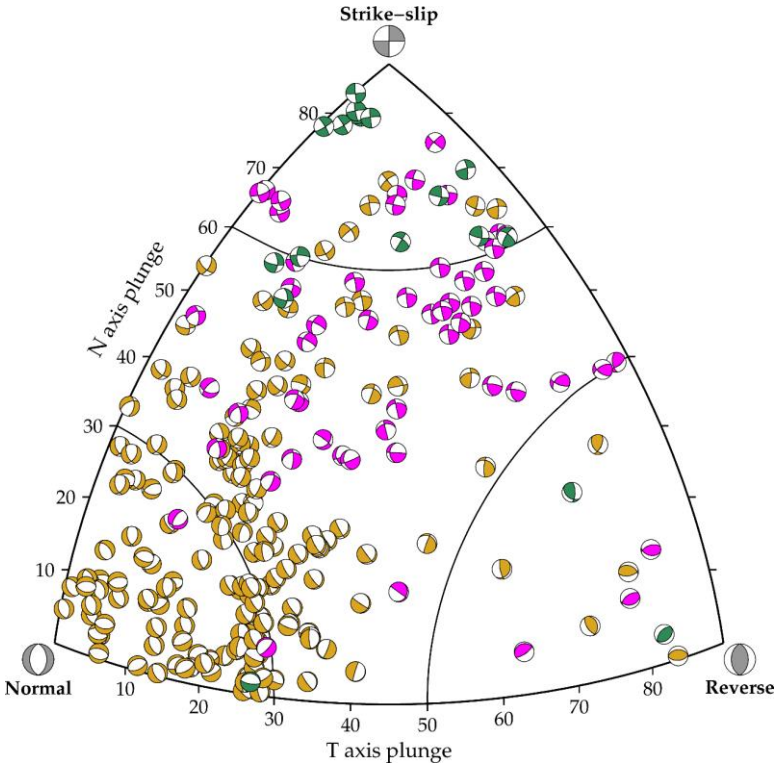

Figure 10. *A Frohlich mechanism categorisation plot (Frohlich, 1992), for all 241 double-couple focal mechanisms displayed in Figure 9. The Frohlich plot is a triangle diagram where the vertices represent normal, strike-slip and reverse focal mechanisms. The different colours refer to the colouring of each geothermal area, as in Figure 9.*

4.1 Krafla

Figures 11 and 12 show the 168 well constrained double-couple focal mechanisms calculated for Krafla during the study period, in map view and the Frohlich categorisation of each event. As before, focal mechanisms in Krafla, particularly within the well field, are dominated by normal faulting to oblique normal faulting (red and yellow colours in Figures 11 and 12), with steep P-axis and shallow T-axis plunge (red and blue dots, respectively, bottom panel in Figure 9). This indicates that most of the normal faults are near vertical, and is in agreement with the catalogue of well constrained focal mechanisms calculated for Krafla from 2018 to 2023, with a total of 856 events (Guðnason et al., 2023a; 2023b). Compared to Þeistareykir and Námafjall, much fewer strike-slip and oblique strike-slip events are observed, meaning that the stress regime in Krafla is very different to both areas, as expected due to the caldera regime.

Looking at the Krafla well field and fissure swarm separately (Figure D1 in Appendix D), and comparing with the time evolution of focal mechanisms within the Krafla well field from 2018 to 2022 presented in Guðnason et al. (2023b), we observe as before a change in the P- and T-axes distribution within the well field, indicating a change in the local stress field. This observation raises the question if the change within the well field is related to the geothermal utilisation, changes in permeability or due to natural variations, since the network geometry has remained the same?

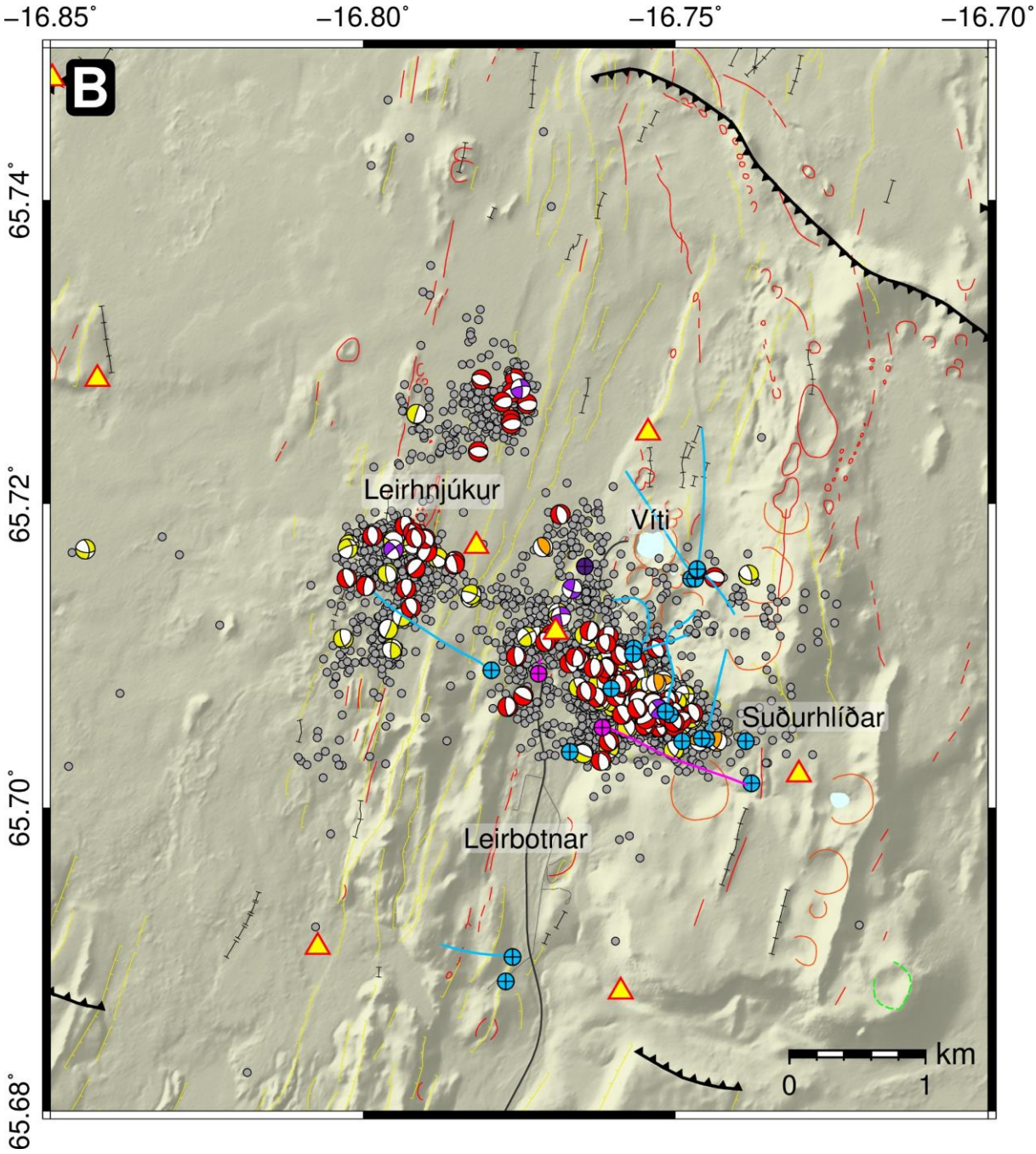

Figure 11. *Map view of double-couple focal mechanisms for 168 selected events in the Krafla geothermal area during the study period, which are dominated by normal faulting to oblique normal faulting. The different colours refer to the colouring for each focal mechanism type (see Figure 12).*

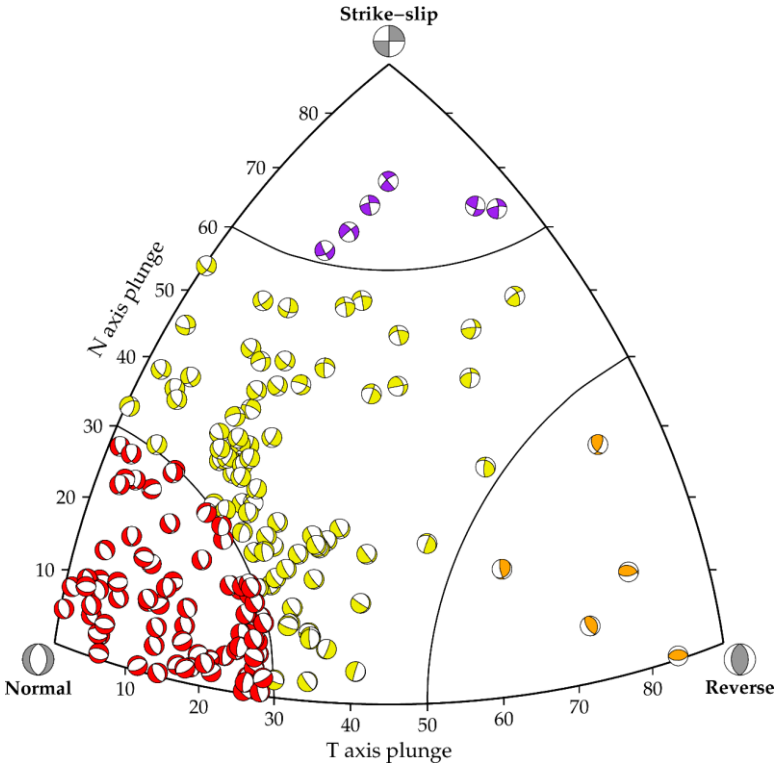

Figure 12. *A Frohlich focal mechanism categorisation plot for the 168 double-couple focal mechanisms in Krafla, displayed in map view in Figure 11. The different colours refer to the colouring for each focal mechanism type.*

4.2 Þeistareykir

Figures 13 and 14 show the 55 well constrained double-couple focal mechanisms calculated for Þeistareykir during the study period, in map view and the Frohlich categorisation of each event. Focal mechanisms are substantially fewer than calculated last year due to lower seismicity rate during the study period, mainly within the Tjarnarás and Randir/Hitur clusters. Different to Krafla, focal mechanisms in Þeistareykir are dominated by strike-slip to oblique strike-slip faulting, mainly confined to the Mt. Bæjarfjall cluster (purple and yellow colours in Figures 13 and 14). This is in agreement with the catalogue of well constrained focal mechanisms calculated for Þeistareykir from 2017 to 2023, with a total of 373 events (Guðnason et al., 2023a; 2023b).

Two normal faulting events are observed, one within the Randir/Hitur cluster as commonly observed, and the other one at the northernmost part of the Mt. Bæjarfjall cluster. Similar to last year, reverse faulting events are observed at the southernmost part of the Mt. Bæjarfjall cluster, below the bottom of the recently drilled well, ÞG-19 (Figure 13).

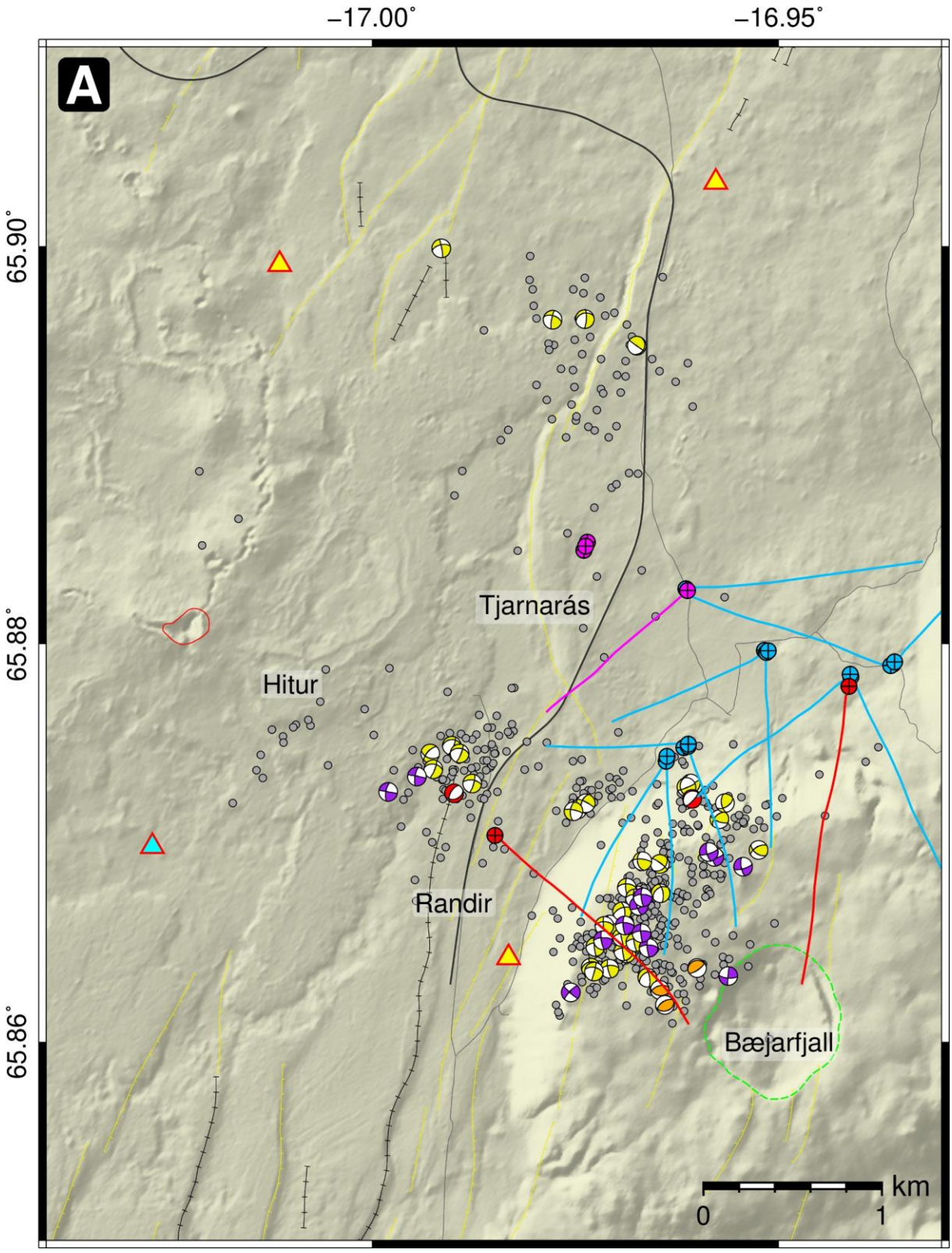

Figure 13. *Map view of double-couple focal mechanisms for 55 selected events in the Þeistareykir geothermal area during the study period, which are dominated by strike-slip to oblique strike-slip faulting, mainly within the Mt. Bæjarfjall cluster. The different colours refer to the colouring for each focal mechanism type (see Figure 14).*

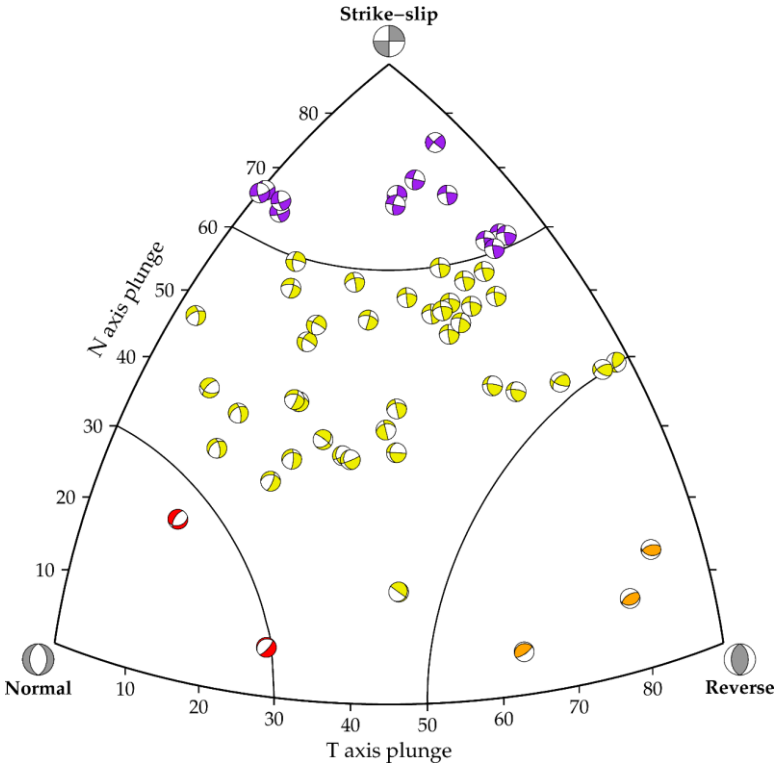

Figure 14. *A Frohlich focal mechanism categorisation plot for the 55 double-couple focal mechanisms in Þeistareykir, displayed in map view in Figure 13. The different colours refer to the colouring for each focal mechanism type.*

4.3 Námafjall

Figures 15 and 16 show the 18 double-couple focal mechanisms calculated for the Námafjall area during the study period, in map view and the Frohlich categorisation of each event. In Námafjall, the focal mechanisms are less constrained than in Krafla and Þeistareykir, mainly due to the sparse station coverage. Due to the network configuration, focal mechanisms in Námafjall can quite easily shift between oblique strike slip and reverse earthquakes as the nodal planes are not tightly constrained.

Focal mechanisms in Námafjall are dominated by strike-slip faulting (purple colour in Figures 15 and 16), likely dominated by the fissure swarm. This is in agreement with the catalogue of focal mechanisms previously calculated for Námafjall from 2019 to 2023, with a total of 41 events (Guðnason et al., 2023a; 2023b).

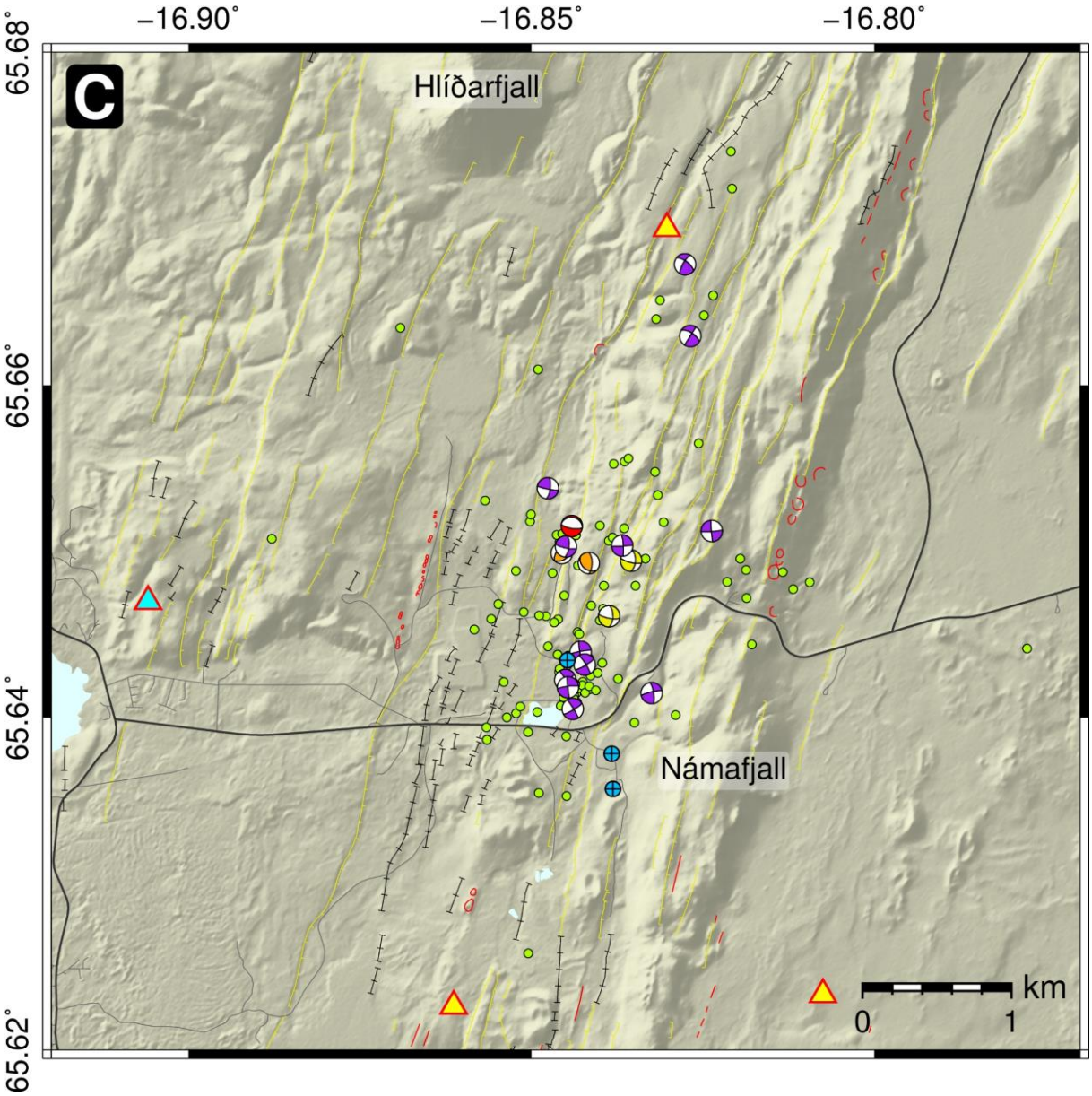

Figure 15. *Map view of double-couple focal mechanisms for 18 selected events in the Námafjall geothermal area during the study period, which are dominated by strike-slip faulting. The different colours refer to the colouring for each focal mechanism type (see Figure 16).*

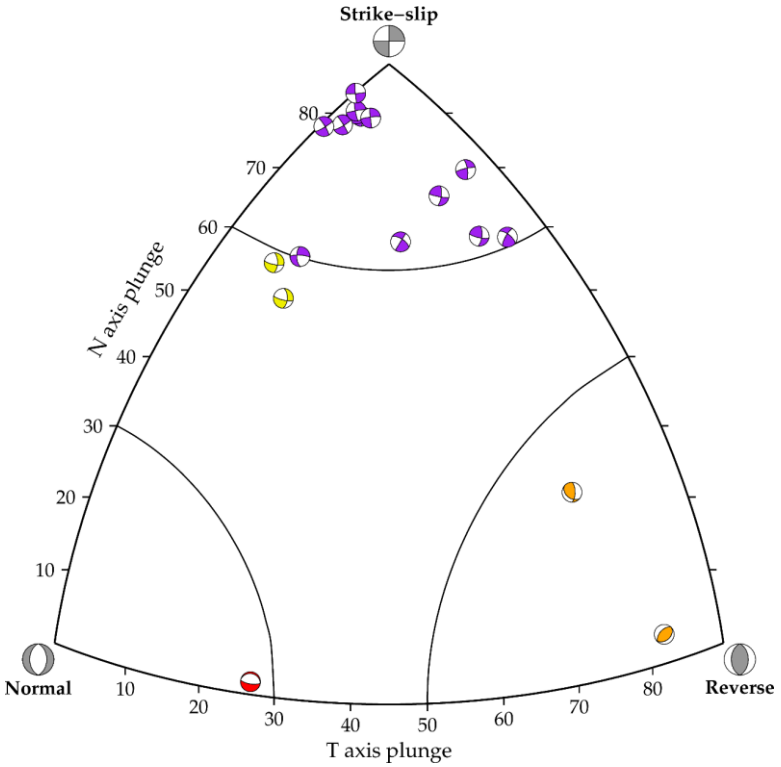

Figure 16. *A Frohlich focal mechanism categorisation plot for the 18 double-couple focal mechanisms in Námafjall, displayed in map view in Figure 15. The different colours refer to the colouring for each focal mechanism type.*

4.4 Non-double-couple earthquakes

Earthquakes caused by a volumetric change, instead of shear slip, are referred to as non-double-couple in the literature. During the study period, 18 earthquakes in Krafla are observed which are consistent with a non-shear faulting behaviour (Figure 17). Event magnitudes are in the range of M_L -0.13 to 0.85. An earthquake is only classified as pure non-double-couple if all P-wave polarities are identical, i.e., either positive or negative. These are non-shear faulting mechanisms that involve either positive or negative volume change, referred to as explosive (positive P-wave polarities) and implosive (negative P-wave polarities) events, respectively. Out of 18 earthquakes, 11 are implosive and 7 are explosive. Four implosive events are observed where one P-wave polarity is non-identical to the rest, and thus, identified as a non-double-couple event, as it did not fit a double-couple inversion.

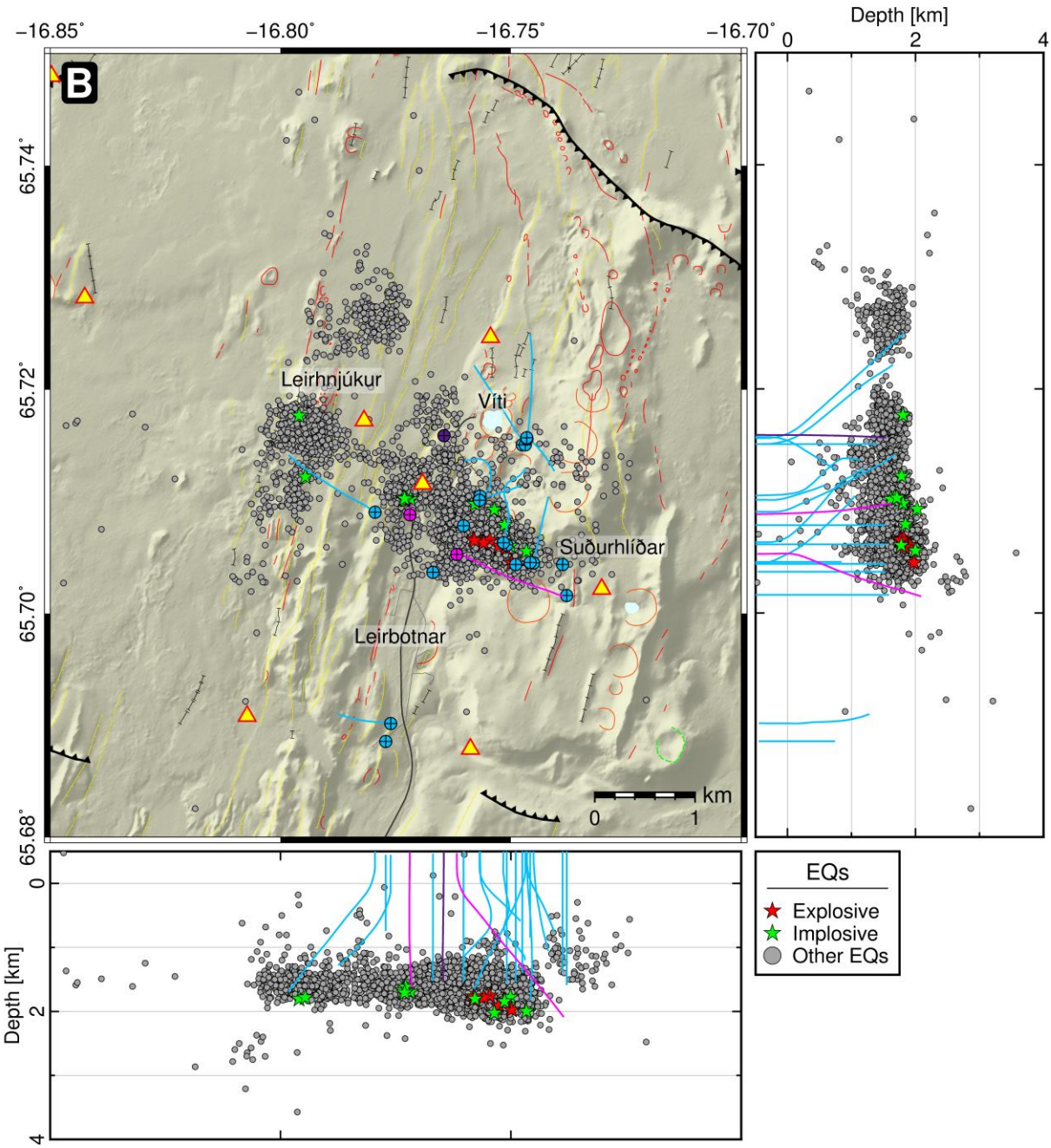

Figure 17. *Non-double-couple earthquakes in the Krafla geothermal area (box B in Figure 1) during the study period, in map and depth view. Explosive events are marked with a red star, and implosive events are marked with a green star. Background seismicity during the study period is shown in grey colour.*

Non-double-couple earthquakes in Krafla have been studied in detail since 2020 (Guðnason et al., 2023a; 2023b). During the study period, fewer non-double-couple earthquakes were observed, compared to last year (35 events in Guðnason et al., 2023a). The majority of events are observed within the cluster confined to the Krafla well field, while only two implosive events are observed within the Krafla fissure swarm. As observed between 2020 and 2023 (Figure E1 in Appendix E), there are two interesting observations from Figure 18;

i. All non-double-couple earthquakes observed in Krafla occur at the deeper end of the depth range, i.e., close to or at the brittle-ductile transition, or the expected melt-rock interface. This suggests that geothermal fluids play an important role in their source processes.
ii. The explosive and implosive events are divided between the southern and northern part of the Krafla well field cluster. This division, also observed by Schuler et al. (2016), suggests some changes within the geothermal reservoir, which needs further study. The division between the southern and northern part of the Krafla fissure swarm, observed in previous years (Guðnason et al., 2023b), is not observed during the study period.

The total of 102 non-double-couple earthquakes observed in Krafla from 2020 to 2024 are shown in Appendix E (Figure E1). All non-double-couple earthquakes in Krafla occur at a depth where geothermal fluid can change the stress locally, and cracks may either open (explosive) or close (implosive).

5 Vp/Vs ratio

The Vp/Vs ratio for the Krafla, Þeistareykir and Námafjall geothermal areas is estimated using standard Wadati diagrams (Wadati, 1933). In a Wadati diagram, the difference of the S- and P-wave travel times is plotted as a function of the P-wave travel time. The relationship between the two should be linear, and the slope of the best fitting line, determined with linear regression, gives a reasonable estimate of the Vp/Vs ratio in the sampled crust for each geothermal area (Figure 18). The ratio averages over the whole travel paths of seismic waves for individual earthquakes. To ensure that the calculated Vp/Vs ratio is representative of the crust within each area, only earthquakes and seismic stations within each of the marked black boxes in Figure 1 (A-C) are used.

The calculated Vp/Vs ratio during the study period is 1.73 ± 0.01 in Krafla, 1.74 ± 0.02 in Þeistareykir and 1.77 ± 0.11 in Námafjall (Figure 18 and Table 1). The Vp/Vs ratio has been continuously analysed since 2016 (Guðnason et al., 2021; 2023a and references therein) (Table 1). The Vp/Vs ratio during the study period remains the same in Krafla, compared to last year, while the ratio in Þeistareykir and in Námafjall is a little lower and a little higher, respectively. Overall, the ratios in Þeistareykir and Námafjall are a little higher and more variable, varying between 1.72 and 1.77 in Þeistareykir and 1.72 and 1.78 in Námafjall. The ratio in Þeistareykir, and especially in Námafjall, is based on an order of magnitude smaller number of earthquakes than in Krafla. The variations in Þeistareykir and Námafjall, therefore, have to be regarded with caution.

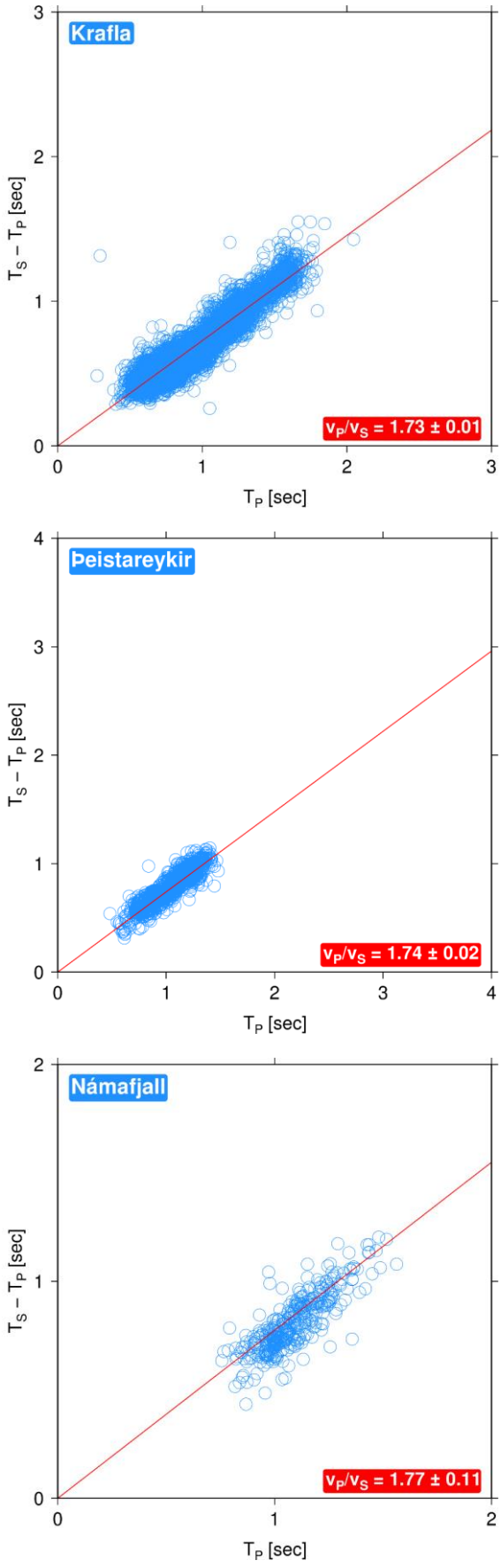

Figure 18. *Calculated Vp/Vs ratio for the Krafla, Þeistareykir and Námafjall geothermal areas during the study period, from top to bottom, respectively.*

Table 1. *Calculated Vp/Vs ratio for the Krafla, Þeistareykir and Námafjall geothermal areas from 2016-2017 to 2023-2024 (Guðnason et al., 2021; 2023a and references therein).*

	Krafla	Þeistareykir	Námafjall
2016-2017	1.70 ± 0.01	1.72 ± 0.02	1.72 ± 0.02
2017-2018	1.70 ± 0.01	1.76 ± 0.01	1.72 ± 0.01
2018-2019	1.71 ± 0.01	1.74 ± 0.01	1.76 ± 0.01
2019-2020	1.71 ± 0.01	1.72 ± 0.01	1.78 ± 0.02
2020-2021	1.71 ± 0.01	1.75 ± 0.01	1.73 ± 0.12
2021-2022	1.72 ± 0.01	1.72 ± 0.01	1.77 ± 0.09
2022-2023	1.73 ± 0.01	1.77 ± 0.01	1.73 ± 0.09
2023-2024	1.73 ± 0.01	1.74 ± 0.02	1.77 ± 0.11

6 Conclusions

Seismic monitoring by Landsvirkjun and ÍSOR of the three developed high-temperature geothermal areas of the Northern Volcanic Zone, NE Iceland; Krafla, Þeistareykir and Námafjall, has provided a large and interesting dataset, i.e., a complete and consistent catalogue of around 74,000 earthquakes, which enables us to reliably look at long term changes in seismicity in all three areas. The main goal is to monitor seismic activity associated with the utilisation of, and re-injection into, the three respective geothermal systems, as well as to monitor natural activity in these volcanic environments.

Results of this year's monitoring are:

- From the 1st of November 2023 to the 31st of October 2024, a total of 4,311 earthquakes were located in the Krafla, Þeistareykir and Námafjall geothermal areas and surroundings, with the highest concentration of earthquakes in Krafla.
- The observed seismicity rate in Krafla and Námafjall is similar to last year, while there is a significant decrease in Þeistareykir within all three clusters, most notably within the Tjarnarás cluster. The decrease coincides with the end of the 2023 inflation episode in Þeistareykir, and is therefore most likely a crustal response to the end of the inflation in the area.
- Micro-seismicity is dominant in all three geothermal areas, with 99% of earthquakes of $M_L < 1.0$, and only two events exceeding M_L 2.0.
- Seasonal variations are observed in i) the seismicity rate in Krafla and Námafjall, with higher rates during the winter months, and in ii) the magnitude range in all three areas, with smaller earthquakes detected during summer, than during winter.
- Double-couple focal mechanisms are calculated for a total of 241 earthquakes, or 168 in Krafla, 55 in Þeistareykir and 18 in Námafjall. Diverse faulting styles are inferred, with

normal faulting dominant in Krafla, while strike-slip faulting is dominant in both Þeistareykir and Námafjall.

- 18 earthquakes in Krafla are attributed to non-double-couple focal mechanisms, both explosive and implosive.
- Compared to last year, the calculated Vp/Vs ratio during the study period remains the same in Krafla, while the ratio in Þeistareykir and in Námafjall is a little lower and a little higher, respectively.
- Activation of the SeisComP waveform cross-correlation location module, *scrtdd*, as part of the automatic event processing system at ÍSOR has resulted in improved automatic locations when compared to the manual catalogue.

References

Ágústsson, K., Guðnason, E. Á., Gunnarsson, K. and Árnadóttir, S. (2011). *Skjálftaverkefnið í Kröflu: Staðan í júní 2011*. Iceland GeoSurvey, short report, ÍSOR-11064.

Árnadóttir, S., Mortensen, A. K., Gautason, B., Ingimarsdóttir, A., Massiot, C., Jónsson, R. B., Sveinbjörnsson, S., Tryggvason, H. H., Egilson, Þ., Eiríksson, J. E. and Haraldsson, K. (2009). *Krafla – Leirbotnar. Hola KJ-39. 3. áfangi: Borsaga*. Iceland GeoSurvey, ÍSOR-2009/058, LV-2009-128, 170 p.

Drouin, V. (2023). *InSAR monitoring of Krafla, Bjarnarflag and Þeistareykir geothermal areas – 2023 update*. Landsvirkjun, LV-2023-063, 25 p.

Drouin, V. (2024). *InSAR monitoring of Krafla, Bjarnarflag and Þeistareykir geothermal areas – 2024 update*. Landsvirkjun, LV-2024-085, 30 p.

Frohlich, C. (1992). Triangle diagrams: ternary graphs to display similarity and diversity of earthquake focal mechanisms. *Physics of the Earth and Planetary Interiors*, *75*, 193-198. https://doi.org/10.1016/0031-9201(92)90130-N.

Guðnason, E. Á. and Ágústsdóttir, Þ. (2021). *Þeistareykir. Minimum 1D Velocity Model*. Iceland GeoSurvey, ÍSOR-2021/003, LV-2021-002, 36 p.

Guðnason, E. Á., Magnússon, R. L., Vilhjálmsson, A. M., Ágústsdóttir, Þ. and Gunnarsson, K. (2021). *Seismic Monitoring in Krafla, Þeistareykir and Námafjall. November 2020 to November 2021*. Iceland GeoSurvey, ÍSOR-2021/049, LV-2021-053, 56 p. http://gogn.lv.is/files/2021-/2021-053.pdf.

Guðnason, E. Á., Ágústsdóttir, Þ., Magnússon, R. L. and Gunnarsson, K. (2023a). *Seismic Monitoring in Krafla, Þeistareykir and Námafjall. October 2022 to November 2023*. Iceland GeoSurvey, ÍSOR-2023/043, LV-2023-060, 40 p.

Guðnason, E. Á., Ágústsdóttir, Þ., Magnússon, R. L. and Gunnarsson, K. (2023b). *Seismic Monitoring in Krafla, Þeistareykir and Námafjall. Reprocessing of the Entire 2006-2022 Catalogue*. Iceland GeoSurvey, ÍSOR-2023/009, LV-2023-021, 56 p.

Gudnason, E. Á., Drouin, V., Yang, Y., Sigmundsson, F., Ágústsdóttir, Th. and Mortensen, A. K. (2024). Changes in seismicity and observed deformation related to inflation at the Theistareykir high-temperature geothermal field, NE Iceland, in 2023-2024. *EGU24-19913, EGU General Assembly 2024,* Vienna, Austria.

Lomax, A., Virieux, J., Volant, P. and Berge-Thierry, C. (2000). *Probabilistic Earthquake Location in 3D and Layered Models*. In: Thurber C.H., Rabinowitz N. (eds.), Advances in Seismic Event Location. Modern Approaches in Geophysics, vol. 18. Springer, Dordrecht. http://dx.doi.org/10.1007/978-94-015-9536-0_5.

Mortensen, A. K., Egilson, Þ., Gautason, B., Árnadóttir, S. and Guðmundsson, Á. (2014). Stratigraphy, alteration mineralogy, permeability and temperature conditions of well IDDP-1, Krafla, NE-Iceland. *Geothermics*, *49*, 31-41. https://doi.org/10.1016/j.geothermics.-2013.09.013.

Pugh, D. J. and White, R. S. (2018). MTfit: A Bayesian approach to seismic moment tensor inversion. *Seismol. Res. Lett.*, *89* (4), 1507-1513. https://doi.org/10.1785/0220170273.

Schuler, J., Greenfield, T., White, R. S., Roecker, S. W., Brandsdóttir, B., Stock, J. M., Tarasewicz, J., Martens, H. R. and Pugh, D. (2015a). Seismic imaging of the shallow crust beneath the Krafla central volcano, NE Iceland. *J. Geophys. Res. Solid Earth, 120,* 7156-7173. https://doi.org/10.1002/2015JB012350.

Schuler, J., White, R. S., Brandsdóttir, B. and Tarasewicz, J. (2015b). Shallow geothermal and deep seismicity beneath Þeistareykir, NE-Iceland. *Jökull*, *65*, 51-59. https://doi.org/-10.33799/jokull2015.65.051.

Schuler, J., Pugh, D. J., Hauksson, E., White, R. S., Stock, J. M. and Brandsdóttir, B. (2016). Focal mechanisms and size distribution of earthquakes beneath the Krafla central volcano, NE Iceland. *J. Geophys. Res. Solid Earth*, *121* (7), 5152-5168. https://doi.org/10.1002/2016JB013213.

Sæmundsson, K., Hjartarson, Á., Kaldal, I., Sigurgeirsson, M. Á., Kristinsson, S. G. and Víkingsson, S. (2012). *Jarðfræðikort af Norðurgosbelti – Nyrðri hluti, 1:100.000*. Reykjavík, Iceland GeoSurvey.

Violay, M., Gibert, B., Mainprice, D., Evans, B., Dautria, J.-M., Azais, P. and Pezard, P. (2012). An experimental study of the brittle-ductile transition of basalt at oceanic crust pressure and temperature conditions. *J. Geophys. Res.*, *117*, B03213. http://dx.doi.org/10.1029-/2011JB008884.

Wadati, K. (1933). On travel time of earthquake waves. *Geophys. Mag., 7*, 101–111.

Appendix A: The *scrttd* processing module

In February of 2024, a new SeisComP location module, *scrtdd*, was activated as part of the automatic event processing system at ÍSOR, as described in Chapter 3. The module has been developed for LV and the areas of interest in previous years (Guðnason et al., 2023b). This module (the LV module is named *lvrtdd*) reprocesses events discovered by other SeisComP locators, e.g., *scanloc* (the LV module is named *N1scanloc*) by comparing them with a background catalogue of events which consists of ~1000 manually revised events, selected to cover the areas of interest. When an event is discovered by a primary locator it is passed onto *scrtdd*, which finds the nearest neighbours from the background catalogue. The event's waveforms are then cross-correlated with those neighbouring events and the differential travel times are used to relocate the event.

Adding *scrtdd* to the processing pipeline has resulted in improved automatic locations when compared to the manual catalogue. The improvements are visualized in Figure A1 and Table A1. The numbers presented are the distances between automatic and manual solutions for the same event. Generally, the distance to the manual solution is about halved after reprocessing with *scrtdd*.

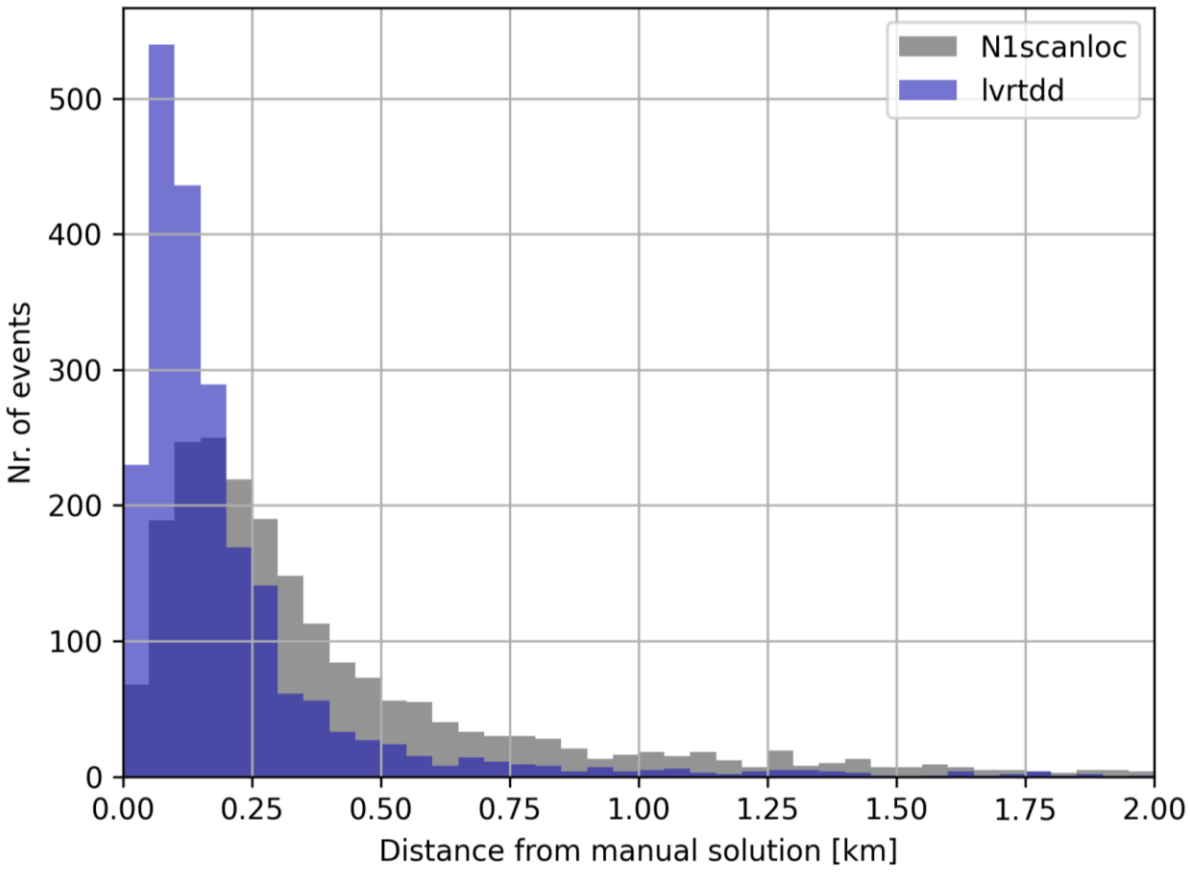

Figure A1. *Histogram showing the distribution of distances for the two location methods, scanloc (N1scanloc) and scrtdd (lvrtdd), during the study period. 2187 events were compared, and the quality was assessed by calculating the distance from the manual event location.*

Table A1. *Distance distribution of the 2187 events compared during the study period for both locators, lvrtdd and N1scanloc. Distances are shown in meters for three different quartiles, i.e., 25, 50 and 75%, referring to Figure A1.*

Quartile	***lvrtdd* [m]**	***N1scanloc* [m]**
25%	79	158
50%	136	280
75%	241	554

Appendix B: Earthquake clusters in Krafla

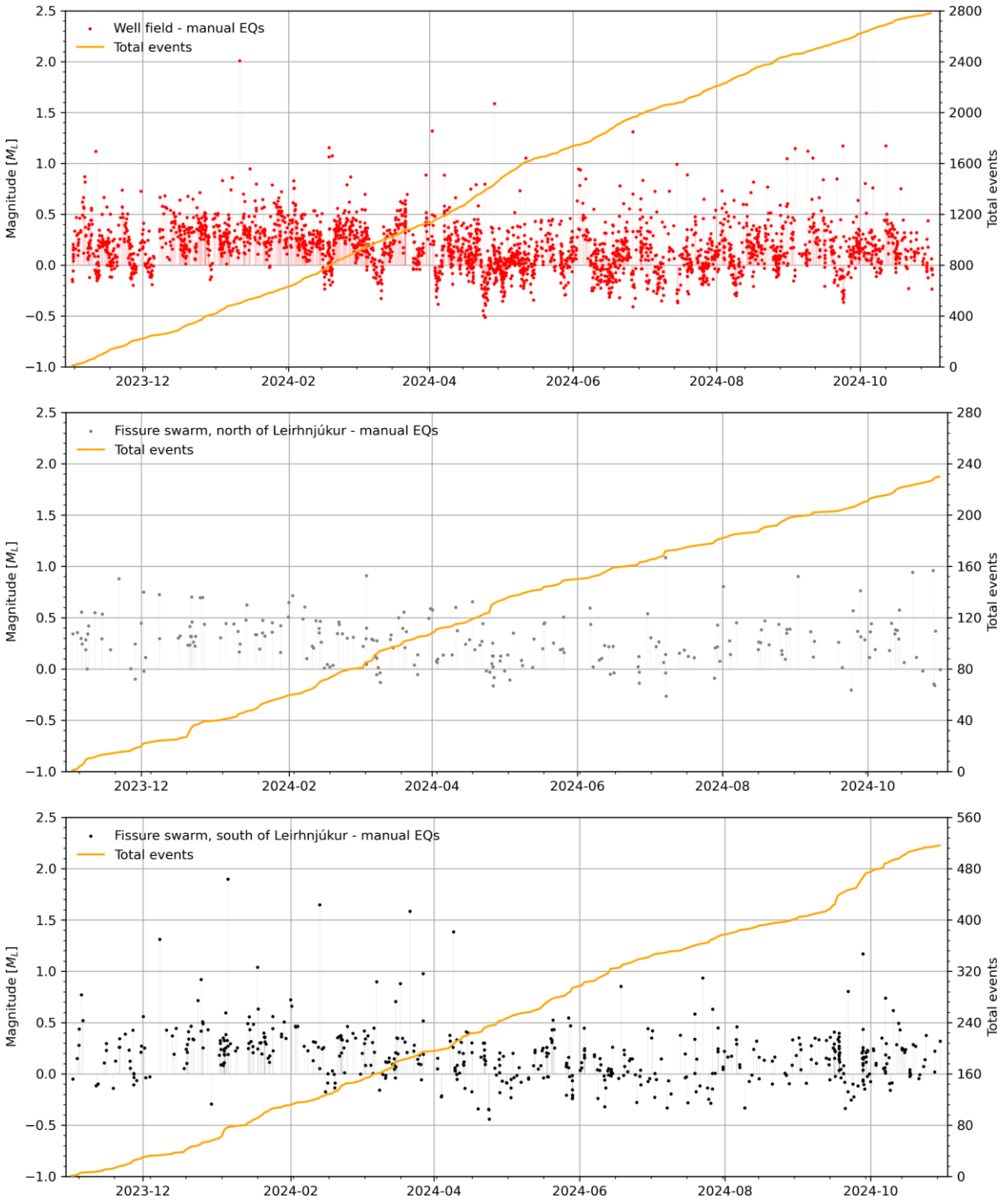

Figure B1. *Time vs. magnitude (M_L) plots of the three different earthquake clusters in the Krafla geothermal area during the study period. Manual earthquakes are shown as different coloured dots; the well field cluster in red (top), the fissure swarm cluster north of Leirhnjúkur in grey (middle) and the fissure swarm cluster south of Leirhnjúkur in black (bottom). The orange line in all plots shows the cumulative number of earthquakes in each separate cluster.*

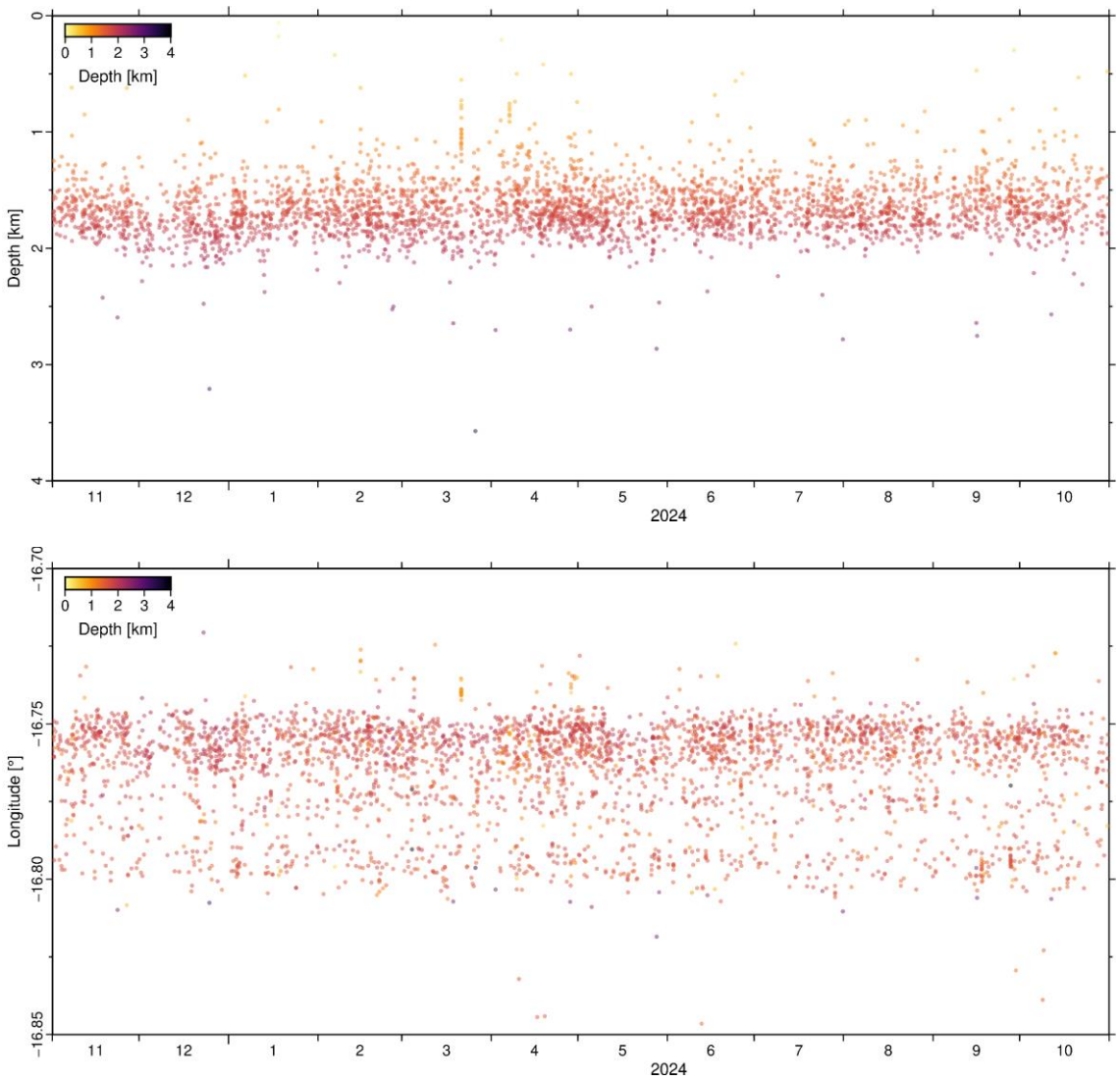

Figure B2. *Time vs. depth (top) and longitude (bottom) of located earthquakes in the Krafla geothermal area (box B in Figure 1) during the study period. Earthquakes are colour-coded by depth.*

Appendix C: Earthquake clusters in Þeistareykir

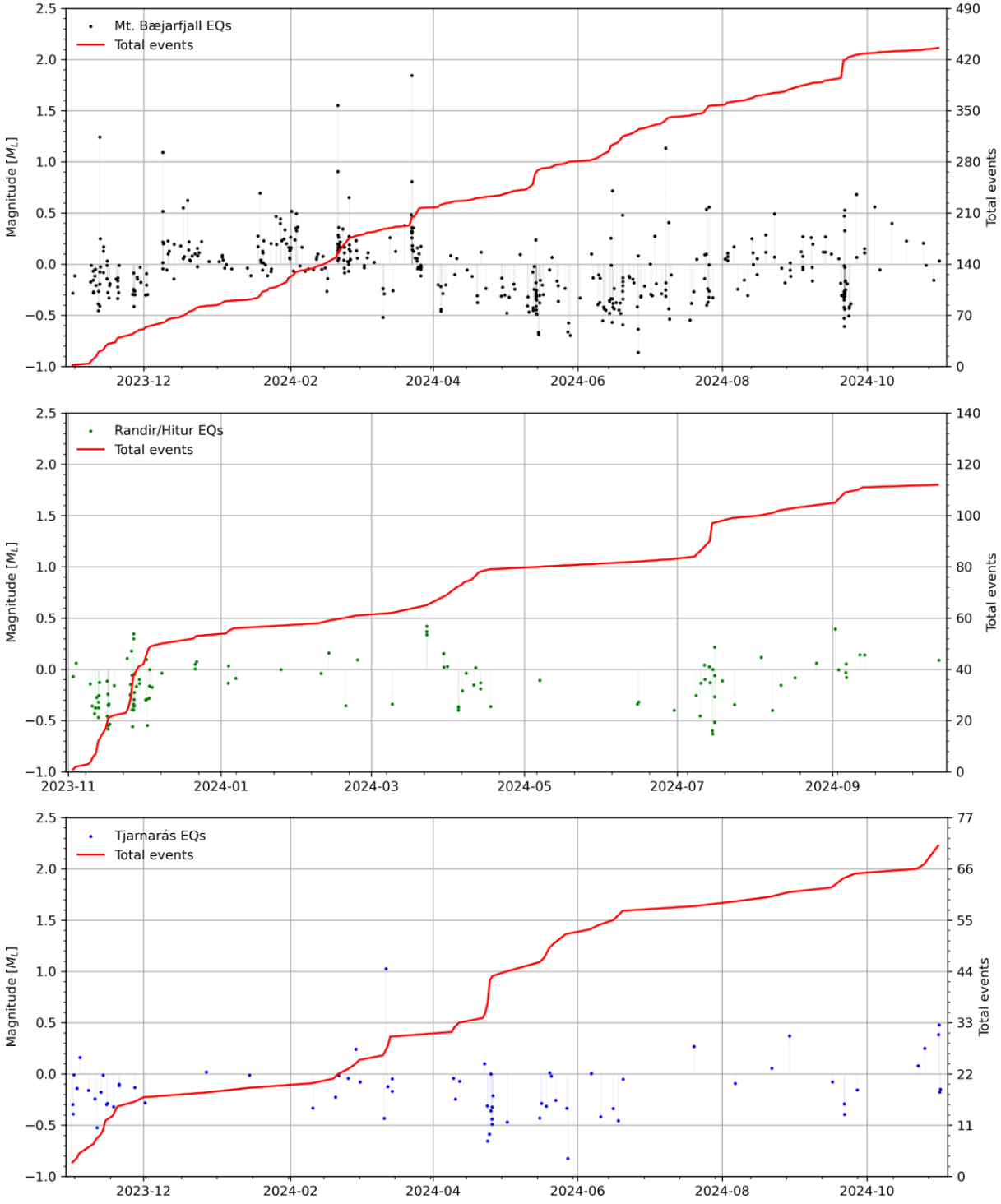

Figure C1. *Time vs. magnitude (M_L) plots of the three different earthquake clusters in the Þeistareykir geothermal area during the study period. Manual earthquakes are shown as different coloured dots; the Mt. Bæjarfjall cluster in black (top), the Randir/Hitur cluster in green (middle) and the Tjarnarás cluster in blue (bottom). The red line in all plots shows the cumulative number of earthquakes in each separate cluster.*

Appendix D: Focal mechanisms in Krafla

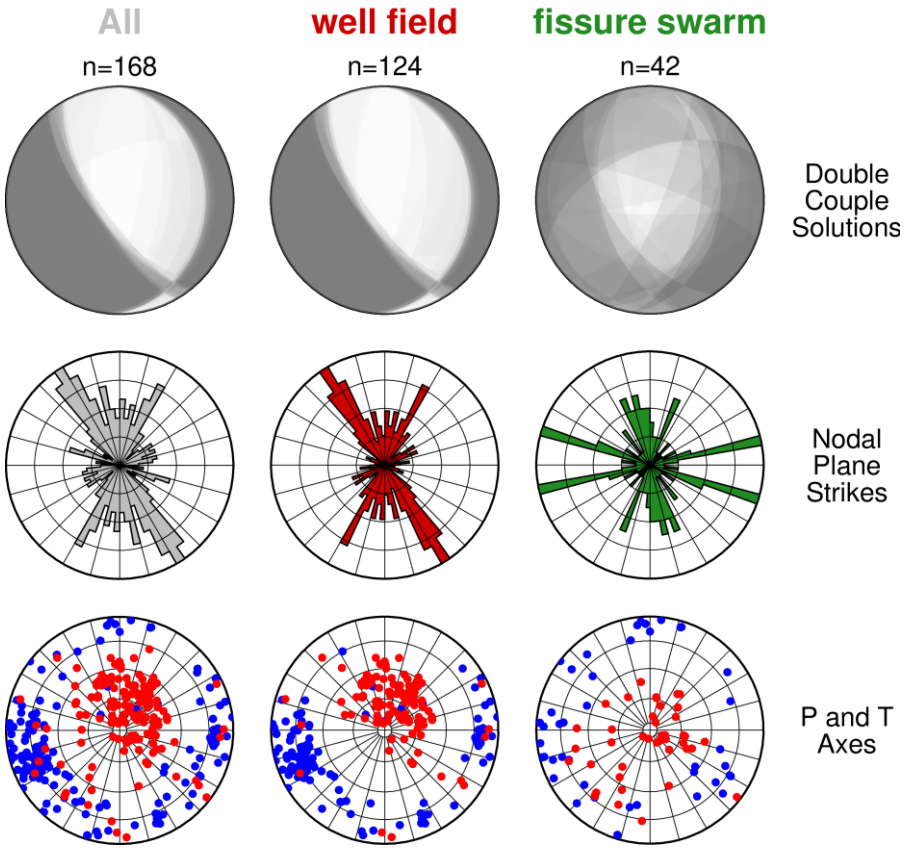

Figure D1. *Graphic summary of all 168 double-couple focal mechanisms located in the Krafla geothermal area during the study period, where n equals number of earthquakes in each group. Krafla is separated into two areas, the well field and the fissure swarm. Top row: all focal mechanisms (white dilatation, grey compression), middle row: strike orientation of all nodal planes, bottom row: orientation of the maximum (P-axis (pressure-axis), red dots) and minimum (T-axis (tension-axis), blue dots) compressive stress.*

Appendix E: Non-double-couple earthquakes in Krafla

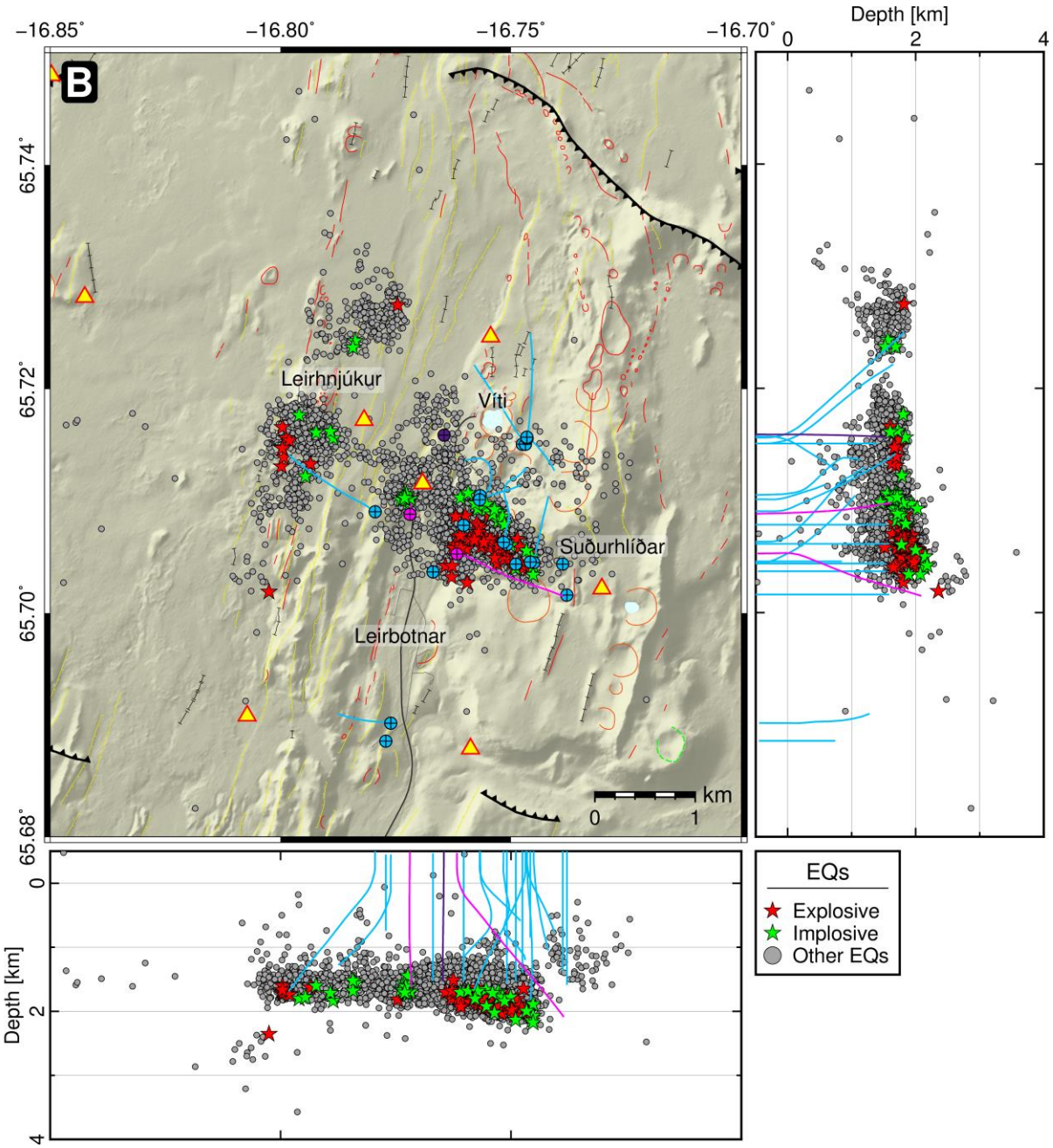

Figure E1. *Non-double-couple earthquakes in the Krafla geothermal area (box B in Figure 1) from 2020-2024, a total of 102 events, in map and depth view. Explosive events are marked with a red star, and implosive events are marked with a green star.*